


 Cite this: *RSC Adv.*, 2025, 15, 31210

# Emergence of shape memory polymers as a new material for diverse applications

 Sravan Kumar Chandaka, Attreyee Das and Partha Laskar \*

The hyper-intelligent features of the shape memory polymers (SMPs) effectively attract the attention of researchers worldwide to translate their potential into a wide range of applications. SMPs possess a unique capability to transform original or predefined shapes to a deformed temporary shape and *vice versa* under the influence of stimuli for instance, water, temperature, light, pH, magnetic field, enzyme, etc. The emergence of SMPs has created a prominent impact in the progress of tissue engineering, drug delivery, designing biomedical devices, electrical/optical sensing, 4D printing, designing deployable devices for spacecraft, wastewater treatment, smart fibres for textiles, etc. However, to translate such smart materials for biomedical and material science applications, there is a continuous hunt of novel polymer functional materials and methodologies to make biocompatible, biodegradable, and adaptable (in chemical and physical properties such as, shape fixity, shape recovery, self-healing, and cross-linking ability etc.) SMPs. The review presents a timely overview of synthesis and diverse applications of functional SMPs in biomedical and material science emphasizing on latest developments and future challenges.

 Received 19th June 2025  
 Accepted 20th August 2025

DOI: 10.1039/d5ra04372g

[rsc.li/rsc-advances](https://rsc.li/rsc-advances)

## 1. Introduction

Mother nature provides endless revelations to researchers to develop innovative solutions to complex problems. Inspired by natural phenomena like the movement of sunflowers towards the Sun, and the opening and closing of the Venus flytrap to catch insects, scientists have developed new synthetic materials that are smart enough to change their structural behavior under external stimuli. These discoveries help to overcome challenges by mimicking living systems (*i.e.* structural and functional alterations under specific stimulations) and advance (bio) materials science and technology.<sup>1</sup> In pursuit of that goal, the evolution of shape memory polymers (SMPs) has been an exciting and emerging area of polymer innovation. SMPs possess a remarkable potential to memorize and regain their actual shape under the influence of external triggers.<sup>2</sup> The natural example of shape memory objects (similar to SMPs) was demonstrated by (Fig. 1) the closing and opening of *Mimosa pudica* (touch me not) leaves upon external stimulations (*e.g.* touch). These remarkable properties make SMPs a versatile candidate for diverse applications in biomedical and material science applications. Furthermore, they can be programmed to adopt multiple temporary shapes and are capable of returning to their original shape under specific stimulus. This unique ability is named as shape memory effect (SME), arising due to

the combined influence of various polymers with distinct chemical compositions under applied programming technology.<sup>3,4</sup> The ability of a SMP material to retain a temporary deformed shape is referred to as shape fixity. It is quantified by the shape fixity ratio ( $R_f$ ), which is the percentage of the temporary shape retained. On the other hand, the ability of a material to return to its original permanent shape, known as shape recovery. It is estimated by the shape recovery ratio ( $R_r$ ), which measures the permanent shape regained.<sup>3</sup> Shape memory cycles involving two distinct shapes are termed as dual-shape effect. Further, shape memory polymers capable of having multiple temporary shapes (*i.e.* memory of multiple temporary shapes) are called multi SMPs. These multi SMPs demonstrate huge advancements in programmability, as shape switching occurs through distinct programming derived from various functionalities of SMPs.

SMPs are further classified into one-way SMPs (1W SMP) and two-way SMPs (2W-SMPs) based on their shape recovery process. 1W SMPs are irreversible, as the shape switching occurs in single cycle and requires reprogramming after every cycle for persistent actuation. For example, thermo-responsive polyurethane (PU) based SMPs, when heated above its transition temperature to attain temporary shape and cooled to retain the deformed shape. Subsequently, reheating above its transition temperature, the PU-SMP recovers its permanent shape. This kind of SMPs generally used for single/limited cycle applications to avoid repeated reprogramming.<sup>4</sup> In contrast, 2W SMPs are programmable to reversible repetitive shape switching between two distinct shapes spontaneously.<sup>5</sup> For example,

Department of Chemistry, GITAM School of Science, Gandhi Institute of Technology and Management (GITAM) Deemed to be University, Visakhapatnam, 530045, Andhra Pradesh, India. E-mail: [laskarpartha@gmail.com](mailto:laskarpartha@gmail.com)



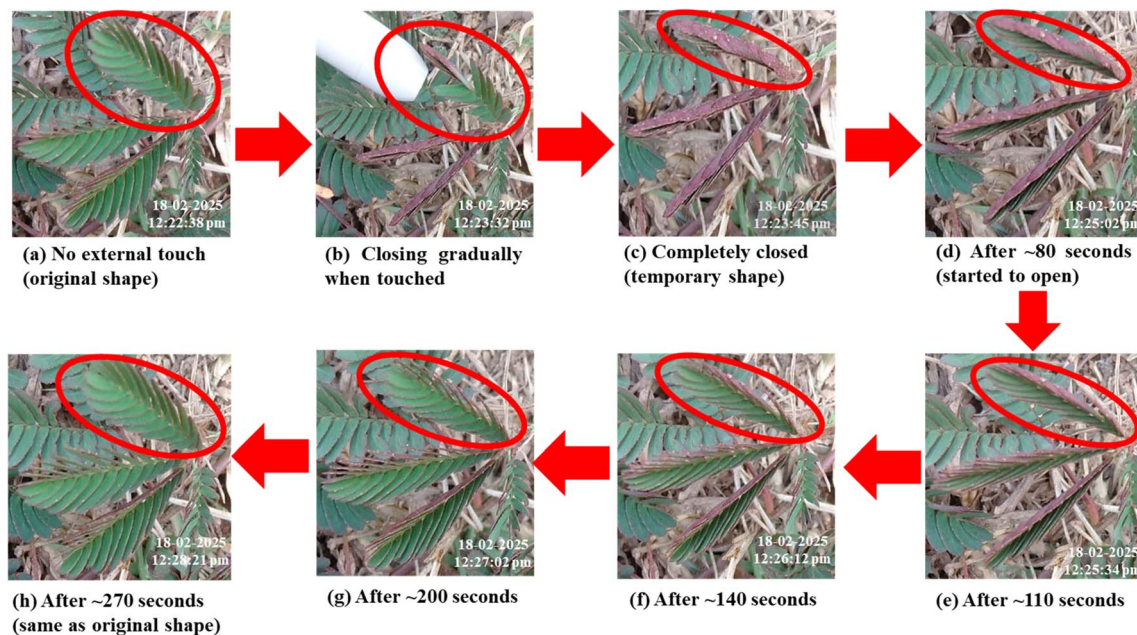


**Fig. 1** Illustration of timely closing and opening reactions of *Mimosa pudica* (touch me not) leaves (highlighted by red circle) upon external stimulation (touch) as a representative example of SMP in presence and absence of stimulus (images were captured by authors on 18th February 2025). Sequence of events: (a) no external touch (original shape); (b) closing gradually when touched (in presence of external stimulus); (c) completely closed (temporary shape); (d) after ~80 seconds (started to open); (e) after ~110 seconds; (f) after ~140 seconds; (g) after ~200 seconds; (h) after ~270 seconds completely opened (same as original shape).

poly(*N*-isopropylacrylamide) is highly soluble in aqueous medium below its lower critical solution temperature (LCST), whereas above LCST (>32 °C) it forms aggregates due to phase transition.<sup>6</sup> Depending on the stimulus, SMP can be divided into various groups such as, thermo-responsive SMPs,<sup>7</sup> light-responsive SMPs,<sup>8</sup> water-induced SMPs,<sup>9</sup> *etc.*

The execution of shape memory effect of SMPs is interlinked with their architecture. The functions like cross-linking density (chemical and physical), backbone flexibility and phase transition behaviour determine their ability of shape fixity, shape recovery and transition temperature.<sup>10</sup> In addition to enhancing mechanical strength, the cross-linkers are also able to induce various stimuli-responsive behaviours to SMPs and make them a potential candidate for multifunctional applications.<sup>10</sup> The higher cross-linking densities helps in enhancing shape fixity; however, it reduces shape recovery due to decrease in mobility of linkers. However, low cross-linking densities enhance shape recovery, but lack mechanical stability.<sup>11</sup> Although, this trend is generally observed for various SMPs, the influence of cross-linking density on shape fixity and recovery can vary depending on SMPs molecular architecture.<sup>12</sup> For instance, polyurethane (PU) based SMPs are composed of hard (*e.g.* hexamethylene diisocyanate) and soft (*e.g.* polycaprolactone) segments. The hard segments determine the shape memory stability and mechanical strength, whereas the soft segments determine the transition temperature. It is found that by incorporating cross-linkers like poly(propylene oxide), polyethylene glycol diacrylate *etc.* with PU, the shape recovery process of SMPs enhances by narrowing the transition temperature range.<sup>13</sup> Further, diels alder (DA) cross linkers also

introduce thermal reversibility to the polymer, which can reform or dissociate in response to temperature and serves as self-healing SMPs, making them as a suitable composite for advanced applications.<sup>14</sup>

SMPs have emerged as an interesting area for modern researchers for past decades, although it flourished much earlier. Vernon *et al.* invented the use of shape memory polymer (specifically methacrylic ester resin) to develop dental materials in the 1940s.<sup>15</sup> Eventually, in the 1960s, the heat shrinkable polyethylene (PEG) (*e.g.*, films of tubing's), was discovered.<sup>15</sup> Thereafter, scientists gradually improved this field by integrating academic research with industrial research by focusing on its underlying mechanism of action and examining their versatile applications in various fields of science and technology.<sup>16</sup> The last 80 years' publication trend in shape memory polymers is clearly indicating a steep rise in research activities for continuous advancement of SMPs (Fig. 2). A few review articles have been published on SMPs, but most of them focused either on very specific application or behaviour based on their structural aspect. For example, some reviews highlighted the molecular architecture of SMPs, while other reviews emphasized mostly on particular biomedical applications such as tissue engineering, drug delivery, stents and self-healing devices, 4D printing for medical applications, and sparsely on aerospace engineering and smart textiles applications.<sup>10,17-23</sup> Thus, the current existing literature is lacking in providing a comprehensive overview about the multifunctional applications of SMP along with structure-property relationship on a single platform. In contrast, this review accumulated diverse applications of SMPs across various disciplines to illuminate





Table 1 List of designed stimuli-responsive SMPs for various applications

Types of applications	Type of SMPs	Types of stimuli	Examples	Year [ref.]
Tissue engineering	Poly( $\alpha,\beta$ -lactide) (PDLLA)- <i>co</i> -trimethylene carbonate (TMC)	Temperature (39 °C)	Bone tissue engineering (calvarial osteoblast)	2014 (ref. 31)
	Polyglycerol dodecanoate (PGD)	Temperature (37 °C)	Soft tissue repair (dorsal skin)	2020 (ref. 32)
	Polyurethane (PU)-polyaniline (PANI)/SiO <sub>2</sub>	Temperature (37 °C)	Cardiac patch (myocardial infraction)	2021 (ref. 33)
	Polyurethane (PU)-ferulic acid (FA)/PU-vanillic acid (VA)/PU- <i>p</i> -coumaric acid (PCA)	Temperature (37 °C)	Wound healing (traumatic wounds like gunshot wounds)	2022 (ref. 34)
	Polyurethane (PU)-poly glutamic acid peptide (PGlu)	Enzyme (V8 enzyme from <i>Staphylococcus aureus</i> )	Chronic wound healing (skin tissue)	2023 (ref. 35)
	Polyurethanes (PU)-poly( $\alpha,\beta$ -lactide- <i>co</i> -glycolide) (PLGA) and polyurethanes (PU)-poly( $\epsilon$ -lactide)/poly ethylene glycol (PLLA/PEG)	Temperature (37 °C)	Rapamycin (human cardiac fibroblast)	2020 (ref. 52)
	DNA-carbon quantum dot (CD)-poly(vinylpyrrolidone) (PVP) hydrogel	pH (7.4)	Hemin (wound healing)	2020 (ref. 53)
	Poly( $\epsilon$ -caprolactone) (PCL)-doxorubicin (DOX)/ $\gamma$ -Fe <sub>2</sub> O <sub>3</sub>	Alternating magnetic field	Doxorubicin (human osteosarcoma)	2021 (ref. 54)
	Polyurethane (PU)-doxorubicin (DOX)-6-mercaptopurine (6MP)/Fe <sub>3</sub> O <sub>4</sub>	Alternating magnetic field	Doxorubicin/6-mercaptopurine (anti-cancer therapy)	2022 (ref. 55)
	Luteolin phospholipid complex (LPC)-polylactic acid (PLA)/poly(ethylene glycol) (PEG)/hydroxypropyl methylcellulose (HPMC)/NaHCO <sub>3</sub>	Temperature (37 °C)	Luteolin (gastric cancer)	2024 (ref. 56)
Biomedical devices	<i>tert</i> -Butyl acrylate and poly(ethylene glycol) dimethacrylate based polymers	Temperature (37 °C)	Vascular stent	2007 (ref. 60)
	Glycerol and poly(ethylene oxide) complexed on chitosan films	Water	Vascular stent	2007 (ref. 61)
	Polyurethanes (PU)/poly( $\epsilon$ -caprolactone) (PCL)	Temperature (37 °C)	Vascular stent	2009 (ref. 62)
	Meth(acrylate) based copolymer	Temperature (37 °C)	Occlusion devices	2013 (ref. 63)
	Poly( $\alpha,\beta$ -lactide- <i>co</i> -glycolide) (PLGA) blend coated with crosslinked poly(ethylene glycol) diacrylate (PEGDA) hydrogel	Water, temperature (37 °C)	Occlusion devices	2016 (ref. 64)
	Hexamethylene diisocyanate (HDI), <i>N,N,N',N'</i> -tetraakis(2-hydroxypropyl) ethylenediamine (HPED), and triethanolamine (TEA)	Water, laser light (810 nm)	Occlusion devices	2007 (ref. 65)
	Polyurethane SMPs	Temperature (37 °C)	Neural interface	2019 (ref. 67)
	Methyl acrylate (MA) and isobornyl acrylate (IBoA) crosslinked with 1 wt% poly(ethylene glycol) diacrylate	Water, temperature (37 °C)	Neural interface	2012 (ref. 68)
	Poly( <i>rac</i> -lactide- <i>co</i> -glycolide)	Water, temperature (36 °C)	Neural interface	2016 (ref. 69)
	Poly(lactide- <i>co</i> -trimethylene carbonate) (PLATMC)	Temperature (37 °C)	Neural interface	2020 (ref. 70)
4D printing	Methyl acrylate and isobornyl acrylate undergo cross linking with 1,6-hexanediol diacrylate	Light (400 to 730 nm) and temperature (70 °C)	Shrinkable electronics	2019 (ref. 71)
	Polyurethane-based filaments	Temperature (85 °C)	Self-shrinking staple	2018 (ref. 72)
			Micro robotics and biomedicine	2022 (ref. 73)

Table 1 (Contd.)

Types of applications	Type of SMPs	Types of stimuli	Examples	Year [ref.]
Aerospace engineering	Isobornyl acrylate as main backbone and poly(ethylene glycol) diacrylate for flexibility, and tricyclodecanedimethanol diacrylate for stiffness	Temperature (70 °C and 25 °C for macro and micro structures)	4D printing of complex shapes (e.g., buckminsterfullerene (C60 bulky ball))	2017 (ref. 74)
	<i>tert</i> -Butyl acrylate (tBA) as a monomer and Di(ethylene glycol) diacrylate (DEGDA) as a crosslinker and phenyl bis(2,4,6-trimethylbenzoyl) phosphine oxide (BAPO) as a UV photo initiator	Temperature (65 °C)	Nanorobotics	2016 (ref. 75)
Aerospace engineering	Benzyl methacrylate (BMA) as linear chain builder and three difunctional oligomers, poly(ethylene glycol) dimethacrylate (PEGDMA), bisphenol A ethoxylate dimethacrylate (BPA) and Di(ethylene glycol) dimethacrylate (DEGDMA) as crosslinkers for distinct SMPs	Temperature (65 °C)	Parabolic reflector	2023 (ref. 79)
	Commercially available carbon fiber fabric and epoxy based SMP resins	Temperature (120 °C)	Deployable bending actuators	2023 (ref. 80)
	Epoxy based SMP resins	Temperature (71.4 °C)	Shape memory polymer composite flexible solar array system (SMPC-FSAS)	2022 (ref. 81)
	Shape memory epoxy and polyurethane phase	Temperature (108.7 °C)	Antenna in spacecraft	2018 (ref. 82)
Recyclable use	Carbon-epoxy fabric and polyurethane-based SMP resin	Temperature (70.9 °C)	Deployable space habitats	2019 (ref. 83)
	Carbon fibre reinforced	Temperature (150 °C) and near infrared radiation (808 nm)	Potential applications to fabricate medical devices, flexible electronics like automobile and aerospace parts <i>etc.</i>	2020 (ref. 92)
	Diels-alders crosslinked polyurethane (DAPU)-functionalized reduced graphene oxide (FRGO2) <i>m</i> -Xylylene diisocyanate (XDI)/ureidopyrimidinone bonded with amine (UPy-NH <sub>2</sub> )	Near infrared light	Adsorption of Pb <sup>2+</sup> and Cu <sup>2+</sup> ions in wastewater	2021 (ref. 93)
Wastewater treatment	Cellulose aerogel (CA)-metal organic framework (MOF) with Zn and Co metals	Temperature (80 °C)	Detection of Fe <sup>3+</sup> ions in wastewater	2022 (ref. 97)
	Hydrogel of a mixture of polyacrylic acid (PAA) & polyvinyl alcohol (PVA)	Water	Adaptive heat regulating fabric	2024 (ref. 98)
Textiles	Cotton yarns and poly(ethylene-co-vinyl acetate) (EVA), cross-linker dicumyl peroxide (DCP)	Sodium salt of EDTA (0.3 molL <sup>-1</sup> )	3D self-folding fabrics for dual thermal regulations	2024 (ref. 102)
	Cotton and coolmax yarns with polydimethyl siloxane (PDMS)/titanium oxide (TiO <sub>2</sub> )	Temperature		2025 (ref. 103)



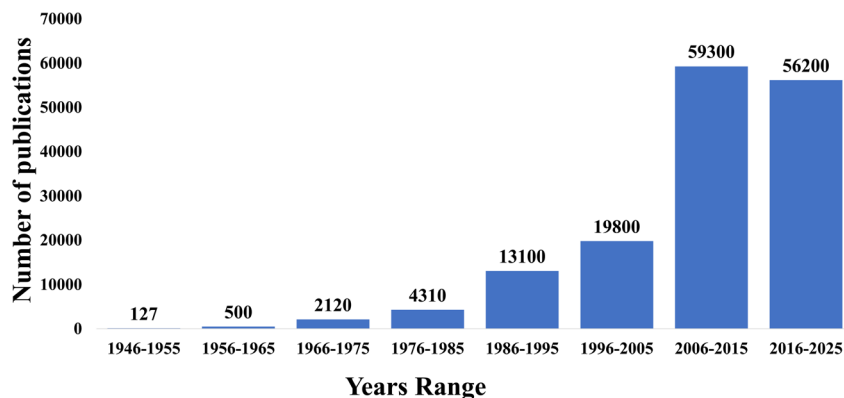


Fig. 2 Publication trends in "shape memory polymer" research. Data from google scholar database searches using keywords: "shape memory polymer". Bar heights represent publication counts for each decade, with totals displayed above each bar. Data analysis conducted on June 9th, 2025.

their potential. Further, progress of such an emerging dynamic cross-disciplinary research area always needs to be addressed in a timely manner. Thus, the review provides an insight about fundamentals of SMPs and their distinct applications over the past decades across a range of disciplines, *e.g.* innovative solutions for biomedical research (including tissue engineering, drug delivery and biomedical devices), smart materials for 4D printing, building next generation spacecraft, solution to environmental problems and fabricating smart textiles (Table 1). Additionally, inclusion of perspective on future challenges and opportunities will offer the readers about the potential of SMPs to be a transformative material from scratch.

## 2. Applications of shape memory polymers

### 2.1 Applications in tissue engineering

Tissue engineering is fundamental to address challenges like tissue damage and organ failure. The traditional treatments methods like organ transplantation have several limitations such as shortage of organ donors, complex healing process and immune rejection.<sup>24,25</sup> To overcome these limitations, scientists have developed smart polymeric materials, which are stimuli responsive and biocompatible.<sup>26</sup> To further improve the efficiency of polymeric materials, SMPs having prominent mechanical properties and precise pore size, in addition to its shape recovery properties were introduced. Thus, these advanced SMPs can be engineered to create scaffolds that promote cell attachment, growth and tissue regeneration at specific tissue sites.<sup>28</sup> Further, SMP-based scaffolds compressed into temporary shape for delivery through a catheter. Once they reach the target site, a specific stimulus is used to trigger them to recover their original shape and provides necessary mechanical strength for cell attachment and tissue growth.<sup>29</sup> Therefore, these materials were utilized for various applications like cardiac repair, bone defect healing, wound healing, soft tissue regeneration *etc.*<sup>27-30</sup> In this section, we have highlighted crucial applications of SMPs in tissue engineering.

Bao *et al.* established a novel fibrous scaffold from SMPs for bone tissue engineering. This fibrous SMP scaffold comprises biodegradable poly(D,L-lactide-co-trimethylene carbonate) (PDLLA-co-TMC) fabricated *via* electrospinning.<sup>31</sup> The studies demonstrated, the composite ratio of DLLA and TMC monomers can be specifically adjusted to 5 : 5, 7 : 3, 8 : 2 and 9 : 1 in PDLLA-co-TMC copolymer to enable fine tuning of glass transition temperature ( $T_g$ ) (19.2 °C to 44.2 °C) for switching shape recovery. Microscopic studies confirmed that the PDLLA-co-TMC fibres (both in 2D and 3D forms) exhibited outstanding shape memory attributes with  $R_f$  and  $R_r$  over 98% and 94% respectively. PDLLA-co-TMC SMPs were found to regain their original shape within  $\sim 10$  s at 39 °C. The bone formation ability was examined by growing rat calvarial osteoblast on fibrous SMP-scaffolds. After 7 days proliferation, *in vitro* studies resulting, an excellent osteoblast adhesion, proliferation and enhanced biomineralization (such as alkaline phosphatase expression and hydroxyapatite like mineral deposition) making SMP-scaffolds an efficient material for bone repair and regeneration applications.

Ramaraju *et al.* developed an advanced biodegradable shape memory elastomer (SMEs) with degradation properties for soft tissue repair.<sup>32</sup> The biodegradable SME, polyglycerol dodecanoate (PGD) utilized in this study, was synthesized by reacting glycerol and dodecanedioic acid at 120 °C under nitrogen conditions for 24 h, subsequently placed under vacuum for 72 h. The polymer poured in silicon moulds to produce specimens with thickness around 2 mm, for that the moulds were preserved in hot air oven for 48 h at 120 °C, 72 h at 120 °C and 48 h at 130 °C for low cure (IPGD), medium cure (mPGD) and high cure (hPGD) respectively with increasing cross-linking densities. Transition temperature was quantified by differential scanning calorimetry (DSC), indicated the decrease in temperature for hPGD ( $34.6 \pm 0.5$ ) when compared to IPGD ( $39.3 \pm 0.2$ ) and mPGD ( $36.9 \pm 0.8$ ), due to increase in cross-linking density. *In vitro* studies were conducted to estimate hydrolytic degradation of PGD in 20 mL of 0.1 mM NaOH over 18 weeks at 37 °C. hPGD demonstrated faster degradation than mPGD and IPGD with near-linear mass loss and significant



degradation observed at 8 and 18 weeks. *In vivo* studies conducted on mice, by placing a patch on dorsal skin demonstrated controlled degradation predominantly by surface erosion. As a result of degradation at the body temperature, the polymers' stiffness increased, making PDG a promising material for implants in minimally invasive soft tissue repair applications.

It's very important to protect the heart from post-operation infections as it may lose tissue extracellular matrix (ECM), which leads to heart failure. So, Feng *et al.* developed an efficient electrospinning submicron fiber cardiac patch to reproduce myocardium ECM and enhance conductive signal transmission for effective myocardial infarction (MI) therapy.<sup>33</sup> The cardiac patch was made using shape memory materials, comprised of polyurethane (PU), polyaniline (PANI) and silicon oxide (SiO<sub>2</sub>). This submicron fiber patch's diameter was in the range of 433.58 to 497.84 nm and thickness of 0.12 to 0.16 mm to effectively stimulate ECM (Fig. 3). These fiber patches exhibited thermo-responsive behavior with strength of 0.11 MPa young's modulus, and elastic degradation around ~106–145% strain, which enhanced mechanical strength to withstand periodic cycles of heart beating. They have studied signal transduction in pig heart slices with patches and evaluated the efficiency of self-adhesion patch on the surface of human neck, finger and wrist. These studies demonstrated morphological stability, conductivity, elasticity for engineering submicron fiber cardiac patches for promising myocardial infarction therapy.

The uncontrolled blood loss and microbial infections in wounds became the leading cause of several traumas related mortalities in the prehospital period. To master this crucial hurdle, Du *et al.* developed modern SMP foams with antimicrobial and antioxidant properties specifically for wound healing.<sup>34</sup> Phenolic acids (PAs) like, ferulic acid (FA), vanillic acid (VA) and *p*-coumaric acid (PCA) were incorporated into polyurethane (composed of *N,N,N',N'*-tetrakis (2-hydroxypropyl) ethylenediamine (HPED) and hexamethylene diisocyanate (HDI) as backbone). The stable FA, VA and PCA foams were synthesized by reacting isocyanate of HDI at 50 °C for 48 h and control foam was synthesized without these acids, to

demonstrate functionality of SMP foams with and without PAs. Phenolic acids-based foams showed uniform morphologies with pore size in the range of 1000 to 1500 nm with enhanced cross-linking. The shape memory of SMP foams examined in wet and dry conditions. These foams were able to recover their shapes at 37 °C within 2 minutes. However, their dry glass transition temperature ( $T_g$ ) is around 55 °C, which makes them stable in secondary(deformed) shape and help them to store at this temperature. The PA-SMP demonstrated notable antioxidant properties by scavenging around 20% hydrogen peroxide and outstanding antimicrobial properties by reducing bacterial colony count in comparison to their respective control foam. All PA-SMP foams not only had greater than 80% cytocompatibility, but also exhibited enhanced platelet attachment and non-hemolytic properties when compared to silver-based controls. This advanced method offers promising results in reducing mortalities by enhancing wound healing, diminishing infections and controlling bleeding effectively.

Ramezani *et al.* developed an innovative bacterial protease responsive SMPs based on polyurethane (PU) for chronic wound healing.<sup>35</sup> Due to the incorporation of polyglutamic acid peptide in PU-based SMPs (PU-Pep) actually triggered to change the shape in presence of bacterial protease. To inhibit the biofilm formation and kill surrounding bacteria, natural antimicrobials (for instance, ferulic acid, cinnamic acid, *p*-coumaric acid) and antibiotic drug (like chloramphenicol) were incorporated in PU-Pep. Synthesized SMPs impregnated with anti-microbials and antibiotic drug showed high shape fixity and shape recovery in range of 74–88% and 93–95% respectively and transition temperature above 60 °C. Shape changing properties of various synthesized PU-Pep SMPs were analysed after a proper incubation with bacteria and mammalian cells, which exhibited shape recovery within 24 h in presence of V8 enzyme originated from staphylococcus aureus (*S. aureus*). The shape changing ability of PU-Pep-antimicrobials SMPs allowed the release of the antimicrobials from SMPs, prevented the biofilm formation on the surface of the samples leading to the reduced tissue damage and aids in chronic wound healing process.

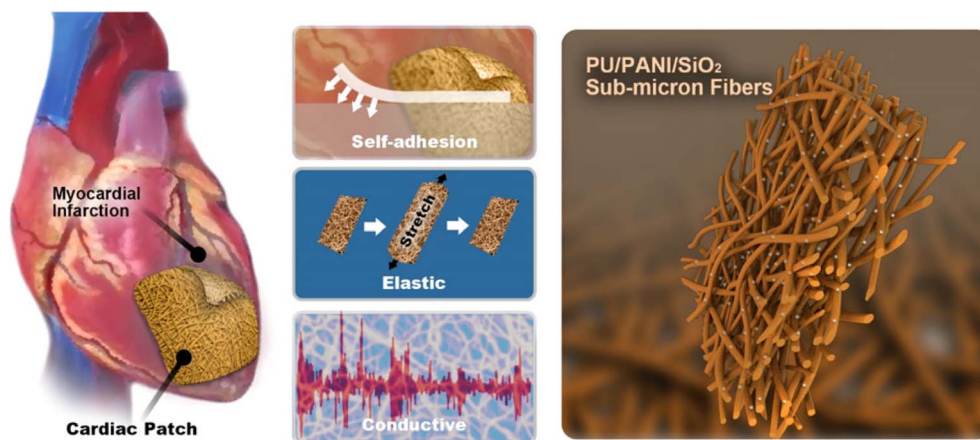


Fig. 3 Representation of submicron cardiac patch for myocardial infarction therapy (reproduced from ref. 33 with permission from ACS Publications, copyright 2021).



## 2.2 Applications in drug delivery

Drug delivery is an important strategy for administering therapeutics to effectively target specific sites in the body by minimizing the toxicity.<sup>36</sup> The aim of this strategy is to improve therapeutic efficacy by overcoming the challenges such as, poor aqueous solubility, non-specific target, low circulation time in the body of therapeutic agents.<sup>37</sup> Over the years, the drug delivery systems transformed tremendously owing to the evolution of smart stimuli-responsive polymer materials in combination with nanomedicine approach.<sup>38,39</sup> The stimuli-responsive systems release drugs by exposure to external triggers (*e.g.* temperature, light, magnetic field *etc.*), which offers a precise control over release of drug at specific location and time.<sup>40–43</sup> For that, significant stimuli-responsive materials were developed for efficient delivery of various hydrophobic and hydrophilic therapeutic agents (like drugs and nucleic acids), utilizing various biodegradable amphiphilic polymers.<sup>44–49</sup> The capability of SMPs to deform and reform their shapes in response to external stimuli is an added advantage to monitor the frequent dosing at tumor sites for elongated time.<sup>50</sup> Thus, SMPs are designed to temporarily adopt a deformed shape for systematic circulation, once exposed to tumor microenvironment it recovers its original shape for controlled release of therapeutic drugs. Further, SMPs can be designed with programmable drug loading and release profiles, which facilitates, on demand and personalized treatment strategies.<sup>51</sup> So, these materials appear to be very prominent in drug delivery applications against cancer, inflammatory diseases *etc.*<sup>50,51</sup> In this section, we have emphasized important studies on targeted drug delivery using SMPs.

It's important to develop SMPs, which are capable of loading drugs to enhance their therapeutic activity for various applications. For example, Bil *et al.* developed an advanced SMPs using shape memory, polyurethane composed of biodegradable polyols for self-fitting grafts as a promising drug delivery system.<sup>52</sup> Two polyurethanes (PU)-based shape memory polymers namely, PU-poly(*D,L*-lactide-*co*-glycolide) (PU-PLGA) and PU-poly(*L*-lactide)/polyethylene glycol (PU-PLLA/PEG) were prepared using ring opening polymerization (ROP). The shape fixity ( $R_f$ ) and shape recovery ( $R_r$ ) of PU-PLGA/Rap were 96% and

99%, whereas  $R_f$  and  $R_r$  for PU-PLLA/PEG/Rap were 91% and 98% respectively. Transition temperatures ( $T_{trans}$ ) of the both SMPs were close to physiological temperature due to their composition. Further, the excellent shape memory features, facilitated the incorporation of anticancer drug rapamycin (Rap). *In vitro* studies of Rap entrapped SMPs demonstrated 79% and 93% of drug release from PU-PLLA/PEG and PU-PLGA respectively for 40 days in PBS solution. *In vitro* studies with human cardiac fibroblast (HCF) cell lines concluded that PU-PLGA/Rap and PU-PLLA/PEG/Rap delivery systems efficiently inhibited cell growth.

Nayak *et al.* developed a novel shape memory hydrogel with poly(vinylpyrrolidone) (PVP), deoxyribonucleic acid (DNA) conjugated with carbon quantum dot (CD) for potential biomedical applications.<sup>53</sup> CD facilitated the cross-linking with PVP and DNA to enhance their mechanical strength, and also helped to introduce outstanding photophysical properties to DNA-CD-PVP hydrogel (Fig. 4). Additionally, the hydrogel was capable of sustained delivery of hemin (used to treat blood disorders like porphyria). The drug release was enhanced at pH 7.4 (97% of hemin was released over 16 days), as the cross-linking density decreased at the physiological pH. CD in hydrogel exhibited antimicrobial activity by generating reactive oxygen species (ROS) upon irradiation with visible light. DNA-CD-PVP hydrogel exhibited ~80% biocompatibility when tested on human fibroblast cells.

SMPs has been successfully developed as an efficient drug carrier in treatment of bone cancer. For example, Ouchi *et al.* reported a shape memory balloon (SMB) to strengthen post-operative chemotherapy and efficient bone cement injection for osteosarcoma.<sup>54</sup> SMB is fabricated with cross-linked poly( $\epsilon$ -caprolactone) (PCL), incorporated with doxorubicin (DOX) and heat generating  $\gamma$ -Fe<sub>2</sub>O<sub>3</sub> magnetic nanoparticles (MNPs). The mechanical properties and crosslinking density of SMB were altered by changing the molecular weight of PCL. The transition temperature of SMB was reported close to ~40 °C leading to 400% shape expansion, which facilitated the injection of bone cement without any leakage. It was found that SMB temporarily memorized its expanded shape at 37 °C allowing the sustained release. Upon exposure to an alternating magnetic field SMB

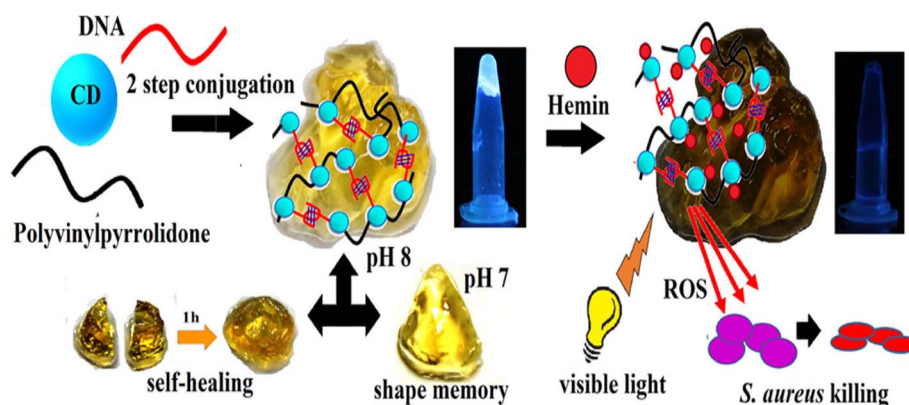


Fig. 4 Representation of conjugation of carbon quantum dot (CD) with DNA and polymer nano material with incorporated hemin and its shape memory properties and drug release kinetics of hemin (reproduced from ref. 53 with permission from ACS Publications, copyright 2020).



demonstrated switchable heating-cooling and thereby released DOX for over 4 weeks, exhibited an elongated effect at tumor site. *In vitro* cytotoxic experiments illustrated that, drug release with heat generation from SMB killed ~99% of human osteosarcoma cells.

Vakil *et al.* reported a novel material for dual drug delivery from a single scaffold with precise delivery profiles.<sup>55</sup> Polyurethane was synthesized using hexamethylene diisocyanate (HDI) as backbone, while polypropylene glycol (PPG) and triethylene glycol (TEG) provided flexibility and hydroxypropyl ethylenediamine (HPED) served as cross linker. Fe<sub>3</sub>O<sub>4</sub> magnetic nanoparticles (MNPs) were incorporated into PU to enable magnetic responsiveness. The SMP was further loaded with drugs or model drug (fluorescent dye), such as, 6-mercaptopurine (6 MP), doxorubicin (DOX) and rhodamine B (Rhod). Applying an alternating magnetic field, MNPs generated heat, which triggered the shape change in SMP and simultaneously drug release. The studies found that cross-linked polymers trapped drugs more effectively than linear polymers, as the cross-linked polymers showed a slower release rate of the drug. These SMPs exhibited cytocompatibility more than 75% for over 72 hours. This novel approach for dual drug delivery minimized side effects and enhanced therapeutic efficacy.

Luteolin has the potential to treat gastric cancer, however its applications were confined by poor aqueous solubility. Zhou *et al.* developed a systematic method for Luteolin incorporated SMPs for gastroretentive drug delivery systems (GRDDS), which enhanced its aqueous solubility, sustained release, biocompatibility, and *in vivo* circulation time.<sup>56</sup> Luteolin phospholipid complex (LPC) was synthesized and incorporated into polylactic acid (PLA) and poly(ethylene glycol) (PEG) based SMPs (PLA/PEG). Among all the prepared SMP films LPC-PLA/PEG (7:3) demonstrated outstanding effectiveness in drug release. Shape recovery analysis of PLA/PEG (7:3) SMPs at 50 °C ( $T_g$  of LPC-PLA/PEG) and 37 °C (Human body temperature) demonstrated 90% and 60% shape recovery respectively within 60 s. Pharmacokinetic studies indicated 354% enhancement of bioavailability in rats when compared to free luteolin. *In vitro* testing of SMPs on SGC-7901 cells demonstrated that the cell proliferation was inhibited by around 89%. In conclusion this study overcame various limitations associated with luteolin and designed a well-organized method for GRDDS.

### 2.3 Applications in biomedical devices

SMP-based biomedical devices are highly advantageous in comparison to traditional metal-based devices. Its adaptive ability helps to complement the surrounding tissues. Moreover, development of biocompatible and biodegradable SMPs allowed researchers to test such smart materials in the preparation of biomedical devices such as vascular stents, occlusion devices, scaffolds for tissue repairing, clot removal devices, surgery suture for wound closure, *etc.*<sup>57</sup>

**2.3.1 Vascular stents.** Vascular stents play a significant role to treat coronary artery diseases. In comparison to metallic stents, SMP based stents are more flexible. They recover to their original shape after being deformed, which helps in

preventing the collapse of small blood vessels.<sup>57</sup> Moreover, they require minimally invasive surgery to implant them in blood vessels as their size can be reduced to the size of the catheter needed for delivery. Further, they offer high controlled deployment at physiological temperature.<sup>58</sup> Considering all these advantages, SMPs are being tested in vascular stents, as the activation temperature for these SMPs is maintained around body temperature. Peripheral vasculature embolization devices (to block or reduce blood flow in specific blood vessels intentionally) incorporating this novel SMP-technology have become a reality and commercially available.<sup>58,59</sup> In this case series, the real time data was collected in the form of post market registry, initial clinical experience to validate these novel devices.

Yakacki *et al.* reported programmable SMPs which can be stored in a catheter, where photo co-polymerization of *tert*-butyl acrylate and poly(ethylene glycol) dimethacrylate was performed to the form thermomechanical responsive SMPs.<sup>60</sup> The fastest recovery of the stent was observed in 10 s for 40 wt% crosslinked stents with a  $T_g$  around 52 °C, in contrast slowest recovery time was observed in 10 min for 10 wt% crosslinked stents with a  $T_g$  around 55 °C.

Chen *et al.* synthesized a biodegradable stent with shape memory property blending glycerol and poly(ethylene oxide) on chitosan films.<sup>61</sup> After blending, the compressive strength of the polymeric stent was increased in comparison to metallic stent. This polymeric stent can withstand up to 30% deformation whereas the marketed metallic stents withstand deformations only up to 10%. Under stimulation of water, the temporary crimped shape converted into fully expanded permanent shape. The polymeric stent recovery time was around 150 s in aqueous medium. *In vivo* studies confirmed that the implanted stent remained intact. However, no thrombus formation was observed in stent-implanted vessels.

Ajili *et al.* reported shape memory polymers using a blend of polyurethane (PU) and polycaprolactone (PCL) polymers with different ratios, which exhibited shape recovery at body temperature.<sup>62</sup> The crystallinity-induced shape memory effect, incorporated the elastic memory in a vascular stent, with alterations in composition and crystallisation conditions, the recovery temperature was attained near the body temperature. For biological applications, the SMP blend (PU/PCL (70/30)) with recovery temperature near body temperature was investigated. *In vitro* studies with human bone marrow stroma cells (hBMSCs cells) demonstrated effective cell adhesion within 3 h and formed dense monolayer after 7 days on SMP blend surface, indicating excellent biocompatibility for the vascular stenting applications.

**2.3.2 Occlusion devices.** Occlusion devices are medical equipment used to close off certain parts of the heart or blood vessels to treat conditions like congenital heart defects and atrial fibrillation (an irregular and rapid heartbeat). It is used to treat these disease conditions instead of open-heart surgery or lifelong medication. Recently, there is a trend to make occlusion devices using biodegradable SMP materials, which can be more customizable and biocompatible than traditional devices.<sup>63</sup> Moreover, the unique property of infiltration of cellular components in SMP foams facilitates to achieve the



large part of the volume occlusion which is difficult to attain using metallic devices.<sup>57</sup> SMP foams fills a void which helps in occlusion. Due to the porous structure of SMP foams, they create a tortuous route for blood to pass through providing multiple sites for recirculation. Moreover, they are easy to implant and rapidly recover their volume after implantation.<sup>64,65</sup>

Xiao *et al.* reported a thermo-viscoelastic model, where they studied the temperature dependent relaxation behaviour of the polymers in presence of low concentrations of water.<sup>63</sup> They synthesized (meth)acrylate-based copolymer network composed of methyl acrylate (MA), methyl methacrylate (MMA), and poly(ethylene glycol) dimethacrylate (PEGDMA) (MA–MMA–PEGDMA) in 5 : 4 : 1 mass ratio respectively. Studies confirmed that water can be used as stimulus, as it diffuses into the MA–MMA–PEGDMA polymer-matrix resulting in the lowering of glass transition temperature. Shape memory behaviour was proven by the full shape recovery of MA–MMA–PEGDMA polymer in 15 min at 50 °C. However, it took 8 hours to get back its original shape at 25 °C and 4 hours at 30 °C.

Wong *et al.* designed a biodegradable water-responsive radiopaque shape memory embolization, where they used a blend of poly(DL-lactide-co-glycolide) (PLGA) and radiopaque filler, followed by further coating with crosslinked poly(ethylene glycol) diacrylate (PEGDA) hydrogel.<sup>64</sup> After getting exposed to body fluid at body temperature, the hydrogel exhibited swelling leading to complete mechanical occlusion. With increase in PEG content in the polymer matrix the glass transition temperature decreased from 42 °C to 36 °C. This filament was found to be very efficient as it recovered its original shape at 37 °C, in presence of water, within 100 s. *In vivo* studies on rabbits confirmed that the embolic device can be delivered *via* a 4F Berenstein catheter into various arteries under general anaesthesia. The initial exposure to body fluid triggered shape recovery, leading to full occlusion within 30 to 120 seconds. Fluoroscopic imaging demonstrated clear visibility of the device due to its radiopaque core.

Small *et al.* fabricated stent-foam device based on SMPs consisting of *N,N,N',N'*-tetrakis(2-hydroxypropyl) ethylenediamine (HPED), hexamethylene diisocyanate (HDI), and triethanolamine (TEA).<sup>65</sup> They were able to attain complete shape expansion at 23 °C under water stimulus within several seconds. The control of deployment was achieved by incorporating epolight 4121 a laser absorbing dye, which was activated at 810 nm. The foam has a density of 0.020 g cm<sup>-3</sup> with 98.4% volumetric void fraction. Differential scanning calorimeter (DSC) studies confirmed that *T<sub>g</sub>* of this foam is near about 40 °C. The preliminary *in vitro* studies (inflammation, thrombogenesis, platelet and neutrophil activation) suggested that this SMP was unlikely to stimulate any negative response.

Rodriguez *et al.* reported a polyurethane based SMP foam and embedded into porcine vein pouch aneurysm model.<sup>66</sup> These materials are easily delivered to the site of action using a catheter due to their flexibility to compression. *In vitro* and *in vivo* studies confirmed their biocompatibility, which was supported by complete endothelial cap at the base and pathological results of the aneurysm. Initial thrombus formation in the foam indicated rapid blood interaction. After 30 days, mild

inflammation and partial tissue connectivity's were observed, and by 90 days' dense connective tissue was observed with minimal inflammation. These studies confirmed that the polyurethane based SMP foam can demonstrate better healing process than bare metal coils in aneurysm occlusion.

**2.3.3 Neural interfaces.** In recent days, advanced treatment of peripheral and autonomic nerves to cure chronic diseases have been proposed. Further investigations have been carried forward with animal cells to find out various treatment methods. Regeneration of the nerves is challenging for the medicos when the peripheral nervous systems are damaged by any accidents and natural disasters. The diameter of nerves is a few hundred μm. Hence, it is difficult to target such small nerves.<sup>67</sup> Thus, stable, biocompatible and implantable neural interfaces are in high demand. Modern SMP-based research may provide a solution to overcome these major difficulties due to their shape-changing features. These SMPs can be engineered to be rigid materials for easy implantation into soft brain tissues, once successfully implanted SMPs triggered by stimulus to soften and recover the shape, which nearly matches with the characteristics of neural tissues.<sup>68</sup>

Zhang *et al.* fabricated a 3D twining electrode, where they combined a stretchable mesh serpentine wire onto an adaptable shape memory substrate.<sup>67</sup> The twining electrode was fabricated by integrating polyimide (PI) film onto synthesized polyurethane based SMP. They used 2D stiff twining electrodes that were temporarily flattened but later grown into nerves which formed 3D flexible neural interfaces at 37 °C to promote the integration with the nerves (Fig. 5). The polyimide (PI) film was reshaped into helical structure during heating at high temperature which facilitated the recovery of the twining electrode. Thus, at 37 °C the flattened electrode self-climbed onto the nerves and recovered its actual helical configuration to make contact with the nerves. It was used in the treatment of nerve injury caused by mechanical and geometrical mismatches and exhibited excellent potential for the electrical neural stimulation.

Ware *et al.* developed a biocompatible thermo and water-sensitive SMP based thin film flexible cortical recording probe, which was fabricated using transfer-by-polymerization method to provide high mechanical and chemical interactions between SMPs and electrode, with least roughness.<sup>68</sup> Methyl acrylate and isobornyl acrylate crosslinked with PEG diacrylate were undergone copolymerization with varying concentrations. Methacrylate polymers contributed to better adhesion between electrodes and polymers. Studies were done by implanting 8 Au recording electrodes and a large ground electrode in the cortex of a laboratory rat.

Chen *et al.* reported a smart nerve conduit (SNC) based on SMPs.<sup>69</sup> Different ratios of co-monomers were tested for polymerization to develop the polymeric network. Variation in co-monomer ratios lead to the variation in shape recovery time. Different polymeric networks with weight ratios of monomers *rac*-lactide:glycolide of PLGA (*e.g.* PLGA-60/40, PLGA-40/60, and PLGA-20/80) were synthesized. In the presence of water, the recovery rate of SNC reached up to 90% after 7 h and attained stability at 36 °C. This relatively slow recovery rate helped to



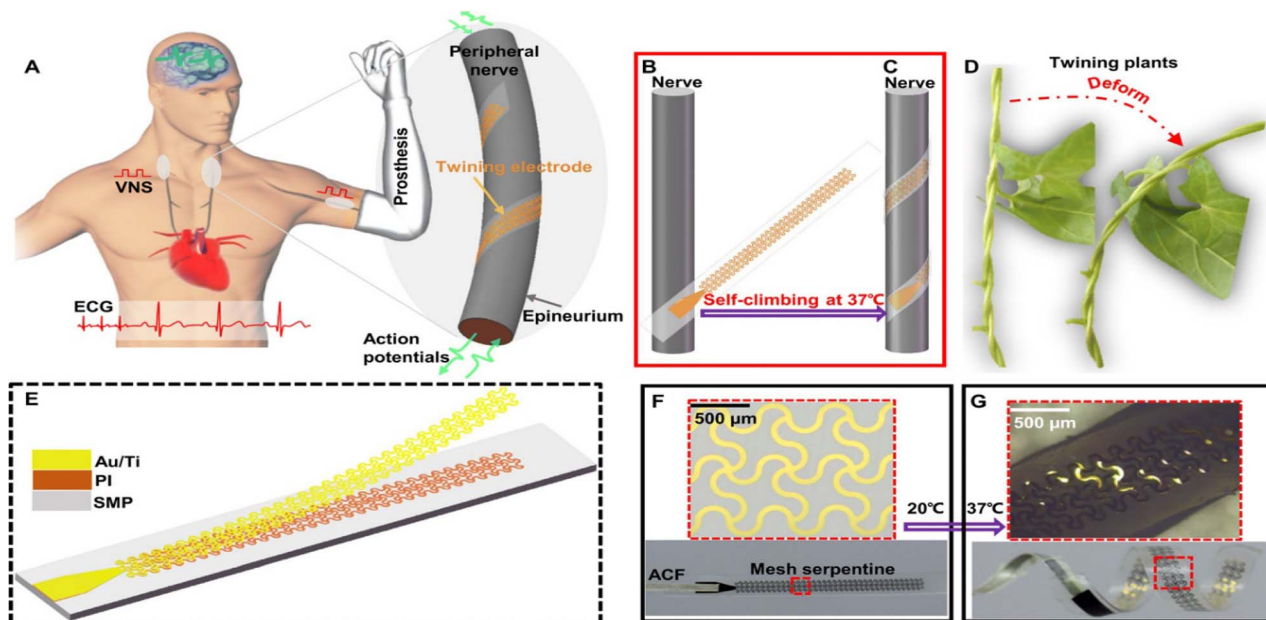


Fig. 5 (A) Pictorial representation of twining electrodes used for peripheral nervous system (PNS); (B and C) self-climbing of SMPs on nerves at 37 °C; (D) representative deformation of the twining plants; (E) design of SMP based twining electrode with Au/Ti and polyimide films; (F) temporary flattened shape of twining electrode; (G) original/ recovered shape of twining electrode (reproduced from ref. 67 with permission from science advances, copyright 2019).

fulfil the requirements in tissue engineering. Cell culture studies were conducted in Schwann cells, which confirmed that poly(*rac*-lactide-*co*-glycolide) copolymers demonstrated satisfactory biocompatibility with negligible cytotoxicity.

Wang *et al.* reported a poly(lactide-*co*-trimethylene carbonate) (PLATMC) SMP-based multichannel nerve guidance conduit for peripheral nerve regeneration.<sup>70</sup> Co-monomers, lactic acid (LA) and trimethylene carbonate (TMC) with different ratios (90 : 10, 70 : 30, and 50 : 50) are fabricated into nanofibers. The  $T_g$  of SMP-nanofiber-based mat was  $\sim 31.62$  °C. Further,  $T_g$  was also found to increase with the increase in LA content in the SMP. It attained a planar temporary structure for cell loading and though under physiological temp (37 °C) it attained a permanent tubular structure. PLATMC displayed good biocompatibility and nerve regeneration potential when studied with a rat having sciatic nerve defect. The conduit provided a favourable microenvironment to assist the process of angiogenesis and vascularization.

#### 2.4 Applications in 4D printing

Combining shape shifting materials and 3D printing have evolved into a new generation called 4D printing. 4D printing adds the fourth dimension (*i.e.* time) to 3D printing.<sup>71</sup> In other words, 4D printing is an advanced 3D printing technique that creates objects, capable of altering their shape, size, colour gradually in response to external triggers.<sup>71</sup> Thus, 4D printing made it easy for digital manufacturing of the complex shapes into smart devices. Various materials like, hydrogel resins, active polymers, or live tissues have been thoroughly investigated as 4D printable smart materials, which are programmed to change their shape in response to environmental factors like

light, temperature, pressure, humidity, *etc.*<sup>72</sup> For the development of such 4D printable smart materials, SMPs have been emerged or exploited to bring a smarter approach in their applications.<sup>72,73</sup> This section emphasized the crucial developments that led to the emergence of 4D printable smart materials.

Zhang *et al.* described a simple digital 4D printing strategy for combining multi SMPs in a single material construct. It provided readily tuneable shape memory characteristics, programmed by light exposure and activated by heating during shape recovery.<sup>71</sup> Isobornyl acrylate (IBOA) and methyl acrylate (MA) underwent cross linking with 1,6-hexanediol diacrylate (HDDA) in the presence of photo initiator bis(2,4,6-trimethylbenzoyl)-phenylphosphineoxide to form the polymer. The co-monomers (IBOA : MA) with molar ratios of 0.71 and 0.62, attained the  $T_g$  at 36–39 °C and 30 °C respectively. Moreover, the bending angle of the resulting polymer beam decreased linearly with increased light exposure time. For example, polymers showed 50° and 0° (*i.e.* non-bending state) bending angle after 14 s and 30 s respectively. Both the SMPs exhibited 100% shape fixity upon light exposure and demonstrated 97.2% to 100% shape recovery respectively under thermal stimulation at 70 °C. These digital SMP can provide nanophotonic behaviour and lead to the deployment of next generation shrinkable electronics.

Triple SMPs (SMP having ability to memorize three shapes) have unique characteristic features to memorize two temporary shapes and recovers to their permanent shape in response to external stimulus. Bodaghi *et al.* reported triple SMPs using 4D printing by incorporating hot-cold programming processes.<sup>72</sup> The polyurethane SMP film with diameter 1.75 mm, exhibited



$T_g$  around 55 °C, excellent shape adaptivity with self-shrinking capabilities. The SMPs in glassy phase demonstrated elastoplastic behaviour at 23 °C, and rubber-like hyper-elasticity at 85 °C. Furthermore, to evaluate the biological relevance, a self-shrinking staple using this SMP was designed and inserted into simulated tissue. At 37 °C, initial recovery of the film was started by gradually closing the gaps like wounds.

Spiegel *et al.* reported a SMP ink system, which was capable of 4D printing at both macroscale and microscale.<sup>73</sup> Digital light processing (DLP) and direct laser writing (DLW) were the appropriate 3D printing techniques to develop such macro and micro systems respectively. SMP was composed of mono-functional isobornyl acrylate as main backbone and crosslinker poly(ethylene glycol) diacrylate for flexibility, tricyclodecanedimethanol diacrylate for stiffness. 4D printed macro and micro structures showed  $T_g$  around 70 °C and 25 °C respectively. DLP printed macro structure demonstrated excellent shape fixity (98%) and shape recovery (97%) ratios (Fig. 6). However, due to small dimensions of DLW printed micro structure, the observation of shape changes with the naked eye was quite challenging. Thus, an optical micro scope with a heating stage was utilized to study, shape changes in micro structures. The results demonstrated faster and complete shape recovery in a double platform micro structure, when heated above its  $T_g$ . Further investigations were made by designing a box-like 4D printed microstructures, which demonstrated potential to trap and release the microspheres under thermal stimulation.

Choong *et al.* reported a dual-component phase switching mechanism-based photopolymer using stereolithography 3D printing technique.<sup>74</sup> SMP was composed of *tert*-butyl acrylate (*t*BA) monomer as main polymer backbone with di(ethylene glycol) diacrylate (DEGDA) as crosslinker (10, 20, 30, 40 and 50 wt%) and phenyl bis(2,4,6-trimethylbenzoyl) phosphine oxide (BAPO) (0.5, 1, 2, 3, 4 and 5 wt%) as a UV photo initiator. SMP exhibited tunable  $T_g$  depending on DEGDA content. For

instance, with 10 wt% of crosslinker SMP showed  $T_g \sim 53.9$  °C, and gradually increase in every 10 wt% of crosslinker,  $T_g$  was increased by around 5 °C. SLA printed SMPs with 10 wt% of DEGBA and 2 wt% of photo-initiator, demonstrated tensile strength of 20.2 MPa and 0.3 MPa at 25 °C and 65 °C respectively. This decrease in tensile strength was due to transformation of SMP from glassy to rubbery state. The SLA-printed SMPs demonstrated outstanding  $R_f$  and  $R_r \sim 95\%$  and 100% respectively. Furthermore, it was able to retain 22 thermo-mechanical cycles, which indicated its high durability. A complex buckminsterfullerene (C60 bulky ball) was 4D printed using this SMP, which demonstrated rapid shape recovery within 11 s in water at 65 °C.

Ge *et al.* reported multimaterial high resolution 4D printing strategy using projection micro stereolithography (PμSL).<sup>75</sup> SMP resin was fabricated with photocurable methacrylate-based monomer; benzyl methacrylate (BMA) as linear chain builders. Three difunctional oligomers, namely poly(ethylene glycol) dimethacrylate (PEGDMA), bisphenol A ethoxylate dimethacrylate (BPA) and di(ethylene glycol) dimethacrylate (DEGDMA) were used as crosslinkers for the formation of three distinct SMP resins. A decreasing trend in  $T_g$  was observed with increase in molecular weight of crosslinker, which resulted in higher stretchability of the copolymer. The copolymer network with BMA and PEGDMA demonstrated high shape fixity and shape recovery ratios (>90%),  $T_g \sim 65$  °C.

## 2.5 Applications in aerospace engineering

Spaceflights with high resolution and communication capability are in increased demand for further progress of space technology.<sup>76</sup> Utilization of SMPs in space engineering has evolved significantly in recent times due to their flexibility, high storage ratio, high frequency and low surface density, which responds to environmental (hostile space environment) stimuli such as temperature or pressure. SMPs can be deformed into temporary shape, which significantly reduces payload for

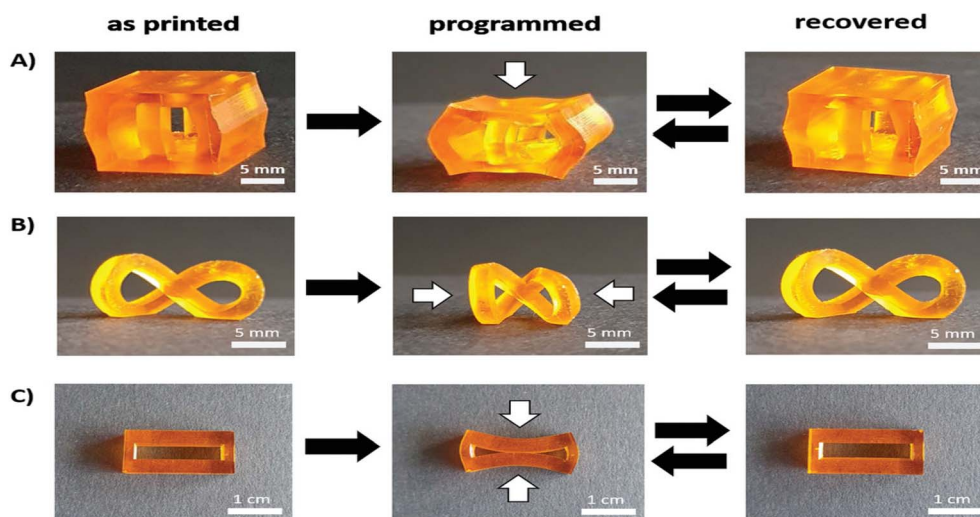


Fig. 6 Shape switching behaviour of multi SMP using 4D printing technology: (A) double platform (B) infinity ring (C) rectangular frame (reproduced from ref. 73 with permission from advanced functional materials, copyright 2022).



launching, upon exposure to stimulus it recovers to original shape.<sup>77</sup> SMPs can be designed to be reversible systems according to the requirement of mission. These SMPs are efficient replacement for complex mechanical systems, as it reduces weight and chance of failure.<sup>76–78</sup> For example, scientists are developing deployable space reflectors to improve carrying capacity, interior space and surface precision.<sup>79,80</sup> SMP are used to build antenna and space habitats to enhance the functionality in space technology.<sup>80–82</sup>

Space reflectors are universally employed in various spacecraft equipment's (e.g. antennas, telescopes, sensing cameras). Traditional deployable reflectors are composed of heavy, complex mechanical architecture for precise opening and closing. Hence, these systems suffer from thermal mismatch issues, as mechanical systems and reflective systems have different coefficients of thermal expansion (CTE). This significantly affects its precision and accuracy, during temperature fluctuations in space. Therefore, reflectors are integrated with SMPs not only to achieve low surface density, but also to enhance storage ratio and frequency. Ming *et al.* fabricated a parabolic reflector using carbon fiber fabric and epoxy based SMP resins with  $T_g$  series of around 100 °C.<sup>79</sup> Using finite element analysis, three folding patterns were compared and finally the six-petal folding pattern was recognized as optimal. It demonstrated an average shape fixation ratio of 95.30%, average shape recovery ratio of 99.37%. The reflector recovered its initial state in around 100 s when the temperature reached up to 120 °C. Thus, these parabolic reflectors demonstrated excellent reliability in laboratory conditions.

Deployable structures require actuators with elevated recovery force to undergo significant volume changes and achieve compact storage for spacecraft. Traditionally, electric motors have been used due to their strong driving force and precise operation. However, their heavy weight and mechanical complexity present challenges. SMPs are considered as promising alternative owing to their light weight for simple actuating process along with their ability to change shape without requiring additional actuators. In this context, Kang *et al.*

fabricated a bending actuator using sandwich structured shape memory polymer composite (SMPC).<sup>80</sup> SMPC bending actuators were fabricated to achieve unique features like, multiple neutral axis (MNA) skins and a deployable core (Fig. 7). The MNA skins were composed of alternating soft and hard layers. The soft layer was fabricated using a composition of polydimethylsiloxane and ethoxylated polyethylenimine. The hard layer was composed of a carbon fabric impregnated on epoxy-based SMP resin with 3 : 1 weight ratio of resin and curing agent. The enhanced shear strain in soft layer reduced the axial strain and consequently enhanced the deformability of SMPC. Therefore, deployment started once the SMPC reached its  $T_g$  (48.4 °C), and initiated the shape recovery process, which was gradually stabilized at 71.4 °C. This SMPC demonstrated highest width along with normalized recovery moment ( $\sim 51.2 \text{ N m}^{-1}$ ) and smallest bending radius ( $\sim 15 \text{ mm}$ ).

Luo *et al.* reported shape memory polymer foam (SMPF), synthesized using SMP based epoxy resin and polyurethane.<sup>81</sup> This SMPF demonstrated high storage modulus ( $2.835 \times 10^7$  at 25 °C) and high compression ratio (sample with 40 mm height compressed to 10 mm at 110 °C). DSC studies confirmed that the  $T_g$  value for SMPF was around 108.7 °C. The SMPF demonstrated outstanding  $R_f$  ( $\sim 99\%$ ), and  $R_r$  ( $\sim 95\%$ ) ratios. The polymer recovered to its initial state in 60 s through heat transfer from electro-thermal film. On 05th Jan 2020, this SMPF was successfully equipped in SMPC-flexible solar array system (SMPC-FSAS), carried by SJ-20 geostationary satellite and successfully deployed in orbit.

Dao *et al.* designed and fabricated a carbon fibre fabric reinforced SMP composite hinge.<sup>82</sup> Dynamic mechanical analyser confirmed the  $T_g$  value of the SMP was 70.9 °C. The key concept involved integration of carbon-epoxy resin with SMPs resin. In this process, the epoxy resin remains in a B-stage (a partially cured epoxy system incorporating a low-reactivity curing agent) after curing, which enhanced both stiffness and shape recovery ratio. Thus, SMP composite was proven to be a suitable candidate to make an antenna for spacecraft.

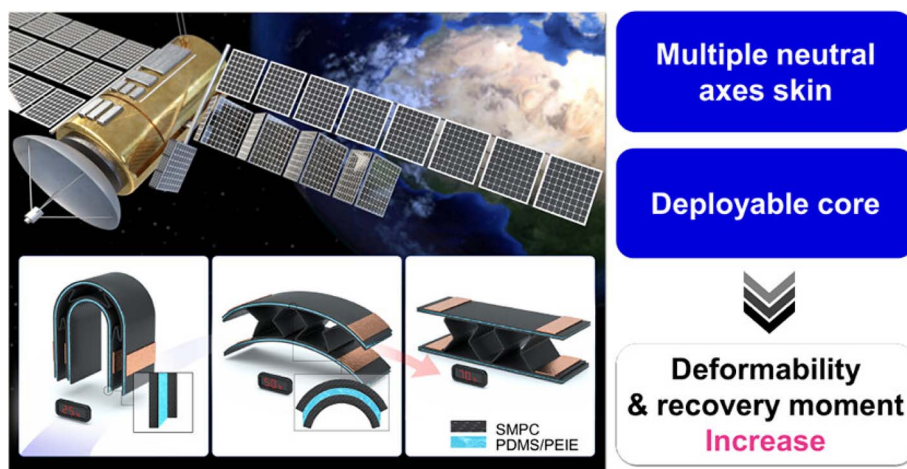


Fig. 7 Schematic representation of sandwich structured SMPC bending actuators and their mechanism (reproduced from ref. 80 with permission from ACS Publications, copyright 2023).



Deployable space habitats are an important part of space research. They have several advantages, such as being lightweight to reduce launch cost, protecting from radiation, expanding the interior space once deployed *etc.* Generally, they are smartly designed to be folded during launch of the spacecraft for efficient storage, followed by the expansion of the structure to create habitable environments in space. Herath *et al.* reported carbon fibre reinforced SMP composites activated by NIR radiation and thermal stimuli for deployable space habitats.<sup>83</sup> These were fabricated on earth, compressed and packed for transport in a spacecraft, and then deployed in outer space to restore their original shape. The SMPC demonstrated 100% shape fixity and 98% shape recovery. Upon stimulation with heated air (150 °C) and NIR (808 nm), it regained its initial shape within 15 s and 50 s respectively. Further improvements were required for this SMPC to be used as efficient deployable space habitats.

## 2.6 Environmental remedies

Polymer waste is a big concern for the environment, particularly synthetic and non-biodegradable polymers. To overcome this, researchers are trying to develop methods to recycle polymeric waste and convert them into some valuable products.<sup>84–86</sup> In this aspect, SMPs waste can also be recycled to reduce any harmful effect on the environment. In addition to this, SMPs are highly useful in detecting some toxic metals present in water, where the traditional methods are inefficient to detect the toxic metals, pesticides present in water.<sup>87,88</sup> Attributed to these features, SMPs play an important role in protecting the environment.

**2.6.1 Recyclable SMPs.** SMPs can be recycled by various methods. However, the challenge is to retain their specific properties like shape fixity, shape recovery, cross-linking ability *etc.*, even after repeated recycling. Recycling SMPs leads to reducing the cost of raw materials to synthesize SMPs and the environmental impact of polymer waste. These recyclable materials have potential applications in fabricating medical devices, flexible electronics for wearable, automobiles, aerospace parts *etc.*, highlighting the significance of recycled SMPs.<sup>89–91</sup> In this section, we have highlighted prominent studies focused on recyclable SMPs.

Du *et al.* reported a novel polyurethane based SMPs with self-healing (SH) and recycling capabilities.<sup>92</sup> Herein, SMPs were composed of diels–alder crosslinked polyurethane (DAPU) integrated with reduced graphene oxide (FRGOs). FRGOs was prepared first by oxidation of graphite to graphene oxide then reduced with hydrazine and functionalized with 2,4-toluene diisocyanate (TDI). DAPU was prepared using poly(tetramethylene ether) glycol (PTMG), polyhydroxyalkanoate (PHA), 2,4-toluene diisocyanate (TDI), chain extender *N*-(2,3-dihydroxypropyl)-maleimide (DHMI) and furan terminated hexamethylene diisocyanate trimer (THDI-FA) as cross linker. DAPU and FRGOs stirred mechanically at 70 °C for 3 h to prepare the composites. DAPU composites containing 1, 2 and 3% wt of FRGOs were named as DAPU-FRGO1, DAPU-FRGO2 and DAPU-FRGO3 respectively. Among them DAPU-FRGO2

exhibited enhanced mechanical and thermal stability due to outstanding thermo-reversibility of DAPU and photo-thermal effect of FRGOs. DAPU-FRGO2 exhibited ~92% and ~94% shape fixity and shape recovery respectively within 10 s under near infrared (NIR) light. To test the recyclability DAPU-FRGO2 was chopped into tiny segments and placed under 20 Mpa pressure and irradiated with NIR light for 10 min. Notably 82–96% mechanical properties of DAPU-FRGO2 were recovered.

Zhang *et al.* reported a temperature responsive SMP, capable of recycling multiple times, had long life and greater thermo-mechanical stability.<sup>93</sup> The shape memory supramolecular polyurea (SMSP) was composed of *m*-xylylene diisocyanate (XDI), ureidopyrimidinone (UPy). SMSP-UPy formed hydrogen bonding and had magnificent shape fixity around 99.5% and shape recovery around 92.7%. It was found that SMSP-UPy film revived its original shape by heating it around 80 °C for 20 s. To test the recycling ability of SMSP-UPy was chopped into tiny segments and hot pressed at 150 °C under 2.5 MPa for 10 min. Even after recycling for 7 times, SMSP-UPy retained its mechanical properties without much decline.

**2.6.2 Wastewater treatment.** SMPs are utilized to treat waste water, where it can adsorb the toxic metals present in water. At present many studies are focusing on developing a prominent SMPs, capable of exhibiting fast and accurate results in detecting heavy metal ions present in waste water.<sup>94–96</sup> For example, SMP based composites are functionalized with various chemical functional groups to efficiently accumulate or bind with heavy metal ions or some toxic pollutants present in the water, followed by the recovery of its actual shape by exposing to temperature, various solvent systems, pH *etc.*<sup>97,98</sup> In this section, we have highlighted important studies focused on SMPs for waste water treatment.

Wang *et al.* reported a shape memory elastic cellulose aerogel (CA) with metal organic frame work (MOF) for adsorption of metal ions in waste water.<sup>97</sup> The aerogel (TPA) was synthesised by blending 2,2,6,6-tetramethylpiperidin-1-oxyl (TEMPO) oxidized-cellulose nanofibers (TOCN) with polyvinyl alcohol (PVA) and citric acid as cross linker. TPA aerogel was soaked in methanol solution, containing Zn (NO<sub>3</sub>)<sub>2</sub>·6H<sub>2</sub>O or Co (NO<sub>3</sub>)<sub>2</sub>·6H<sub>2</sub>O for 10 min, followed by addition of 2-methylimidazole to get zeolitic imidazolate framework-8 (ZIF-8) and zeolitic imidazolate framework-67 (ZIF-67) on aerogel, forming TPAZ-8 and TPAZ-67 respectively. These MOF-aerogels have low density (9.8–11.2 mg cm<sup>-3</sup>), high porosity (~99%) and exhibited shape recovery, up to 80% strain recovery within 1.5 s under-water. The adsorption capabilities of TPAZ-8 were 54.78 mg g<sup>-1</sup> for Cu<sup>2+</sup> and 105.21 mg g<sup>-1</sup> for Pb<sup>2+</sup>, whereas in case of TPAZ-67, 70.53 mg g<sup>-1</sup> for Cu<sup>2+</sup> and 123 mg g<sup>-1</sup> for Pb<sup>2+</sup>. These results demonstrated TPAZ-67 had good adsorption capacity, compared to TPAZ-8.

Li *et al.* reported an easy and economic method for detection of Fe<sup>3+</sup> ions using a shape memory hydrogel.<sup>98</sup> The hydrogel was prepared by using poly acrylic acid (PAA) and poly vinyl alcohol (PVA). The permanent and temporary shape of PAA/PVA hydrogel was due to hydrogen bonding and coordination of metal ions with the carboxyl group respectively. The deformed shape of hydrogel was reverted by immersing it in aqueous



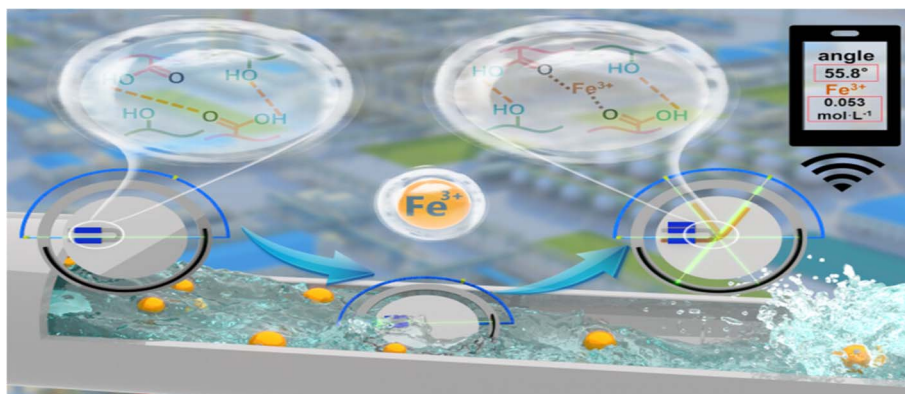


Fig. 8 Schematic representation of detection of  $\text{Fe}^{3+}$  ions in water using shape memory hydrogel (reproduced from ref. 98 with permission from ACS Publications, copyright 2024).

solution having 0.3 mol per L sodium salt of ethylene diamine tetra acetic acid (EDTA). Hydrophilicity and swelling behavior of hydrogel depended on pH, e.g. at  $\text{pH} < 7$  carboxyl groups in hydrogel were protonated; at  $\text{pH} = 7$ , they gradually deprotonated and at  $\text{pH} > 7$  coordination with  $\text{Na}^+$  occurred. The PAA/PVA hydrogel became denser after immersion in water. However, pore size became smaller once hydrogel was immersed in wastewater containing  $\text{Fe}^{3+}$  ion. Shape memory effect with other metal ions such as,  $\text{Cu}^{2+}$ ,  $\text{Cr}^{3+}$ ,  $\text{Al}^{3+}$ ,  $\text{Na}^+$ ,  $\text{Mg}^{2+}$ ,  $\text{K}^+$ ,  $\text{Ca}^{2+}$ ,  $\text{Mn}^{2+}$ ,  $\text{Co}^{2+}$ ,  $\text{Ni}^{2+}$ , and  $\text{Zn}^{2+}$  was studied along with  $\text{Fe}^{3+}$  ion. The results demonstrated the highest shape fixity ratio around 90% for  $\text{Fe}^{3+}$  ion and for other metals shape fixity ratio was around 20%. It was noted that with increase in  $\text{Fe}^{3+}$  ion concentration the shape fixity ratio increased and acted as a portable  $\text{Fe}^{3+}$  ion concentration detector (Fig. 8). PAA/PVA hydrogel was placed in  $\text{Fe}^{3+}$  ion solution and measured the angle of PAA/PVA hydrogel with laser protractor and the smart terminal detected three various concentrations of  $\text{Fe}^{3+}$  ions (e.g. 0.053, 0.016 and 0.004  $\text{mol L}^{-1}$ ). This method of detection was highly helpful to detect  $\text{Fe}^{3+}$  ions in wastewater without any complex instrumentation.

## 2.7 Applications in textiles

The natural, synthetic, and blended fibres are used to fabricate various textiles to serve multiple purposes. Generally, these fibres are composed of cellulose polymer, polyamide, polyester, nylon *etc.*<sup>99</sup> Additionally, these fibres can be also moulded into smart materials by incorporating various cross-linkers such as imine/amine bond, PVA, cyclic anhydrides *etc.*<sup>100</sup> Further, scientists are trying to fabricate shape memory fibres to design novel SMP based textiles for various applications including, clothing, thermal insulator, bandages, masks, *etc.*<sup>101</sup> This section highlighted the latest developments of SMP based fabrics, portraying the significance of SMP for the growth of textile industry to meet evolving human needs.

The massive energy consumption by systems used for indoor temperature controlling through air conditioners (heating/cooling) to maintain a comfortable atmosphere was a critical issue as it leads to greenhouse gas emission. To address these

challenges, Zou *et al.* developed a novel smart textile with reversible gap modulation and unidirectional moisture transport to regulate the temperature of human skin.<sup>102</sup> The SMP textile fabric was composed of thermos-responsive poly(ethylene-co-vinyl acetate) (EVA) as polymer backbone with dicumyl peroxide (DCP) as cross-linker. Cotton yarns with varying thickness and cross-linked EVA were employed to design the SMP-based smart textile. The cross-linked EVA fibres allowed the fabrics to undergo shape switching in response to temperature. With the rise in temperature, the textile exhibited shape recovery leading to the opening of gaps, which eventually enhanced the permeability of air and moisture to release heat and sweat. Sequentially, cooling led to closing the gaps to maintain warmth conditions. The modulated fabric exhibited high  $R_f$  and  $R_r$  around 95% and 98% respectively, with an enhanced air (443.5 to 461.7  $\text{mm s}^{-1}$ ) and moisture permeability (1761.8 to 2021.5  $\text{g d}^{-1} \text{m}^{-2}$ ) than that of the cotton fabric. Further, 1% wt sodium methyl silicate was used to create one side hydrophobic layer for unidirectional moisture permeability (index around 193.2). The hydrophobically coated SMP-based textiles showed a good heat conductivity (0.089  $\text{W m}^{-1} \text{K}^{-1}$ ) along with enhanced air permeability (1600.5–1963.8  $\text{g d}^{-1} \text{m}^{-2}$ ). Thus, the SMP-based cloths could be good replacement for air conditioners leading to reduced carbon emission.

Zhang *et al.* developed a novel 3D self-folding fabric capable for dual mode thermal regulation aiming to serve as personal comforting fabric in varying weather conditions.<sup>103</sup> The fabric was designed using cotton and coolmax yarns using weft knitting to induce spontaneous folding. Then the fabric was coated with polydimethyl siloxane (PDMS)/titanium oxide ( $\text{TiO}_2$ ) in THF solution for two times to obtain optimal reflectance and softness. In warming mode, the modulated fabric demonstrated a 3D folded structure that traps air between the folds, resulted in enhanced insulation and thermal resistance up to 0.0627  $\text{m}^2 \text{K}^{-1} \text{W}^{-1}$ . However, in cooling mode the fabric stretched to obtain a 2D flattened structure resulting 93.5% and 89.5% enhancement of infrared (IR) emissivity (8–13  $\mu\text{m}$ ) and solar reflectance respectively due to the exposed PDMS/ $\text{TiO}_2$  coating (Fig. 9). This 2D flattened structure helped to reduce the temperature of the body up to 4.3–4.9  $^\circ\text{C}$  under sunlight. The



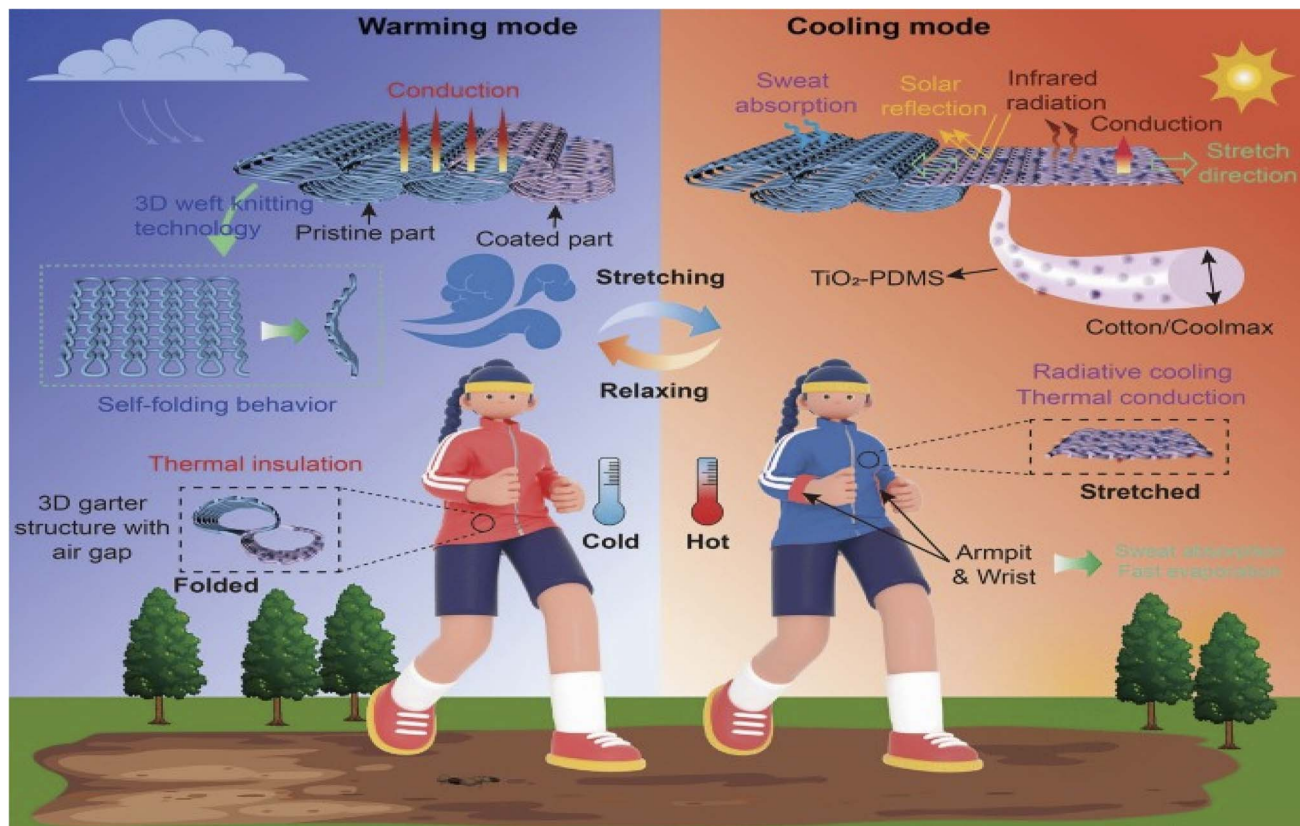


Fig. 9 Schematic representation of dual mode fabric response in warming and cooling condition (reproduced from ref. 103 with permission from Springer Nature, copyright 2025).

fabric demonstrated reliable air permeability ( $22.44 \text{ mL s cm}^{-2}$ ), water absorption (387.89%), water evaporation rates ( $1.182 \text{ g h}^{-1}$ ), durability (over 1000 cycles) and stability after multiple washes. Hence, this dual 3D and 2D structured fabric served as adaptable wearable garments to withstand distinct environmental conditions.

### 3. Conclusion and future perspectives

In conclusion, SMPs are smart, eminent, and programmable stimuli responsive polymeric materials, capable of memorizing multiple shapes and recovers to their initial shape under specific stimulation. There is always a need to synthesize economical, non-hazardous and biodegradable SMPs, which eventually facilitates diverse applications in various fields. In this review, we have summarized synthetic procedures and applications of SMPs for the development of various biomedical devices and biocompatible micro robots using 4D printing. Furthermore, we have discussed their prominence in drug delivery, tissue engineering and waste management. Additionally, we have emphasized, SMPs significance in developing various smart fabrics and deployable devices for spacecraft to enhance their functionality in the space environment. The existing reviews on SMPs mostly focus on specific areas of application. Unlike that, this article provides thorough insight

on versatility and multidisciplinary potential of SMPs across various fields of science and technology.

In our perspective, new age SMPs can be further developed into much smarter materials, so that they illuminate a path to overcome the modern-day challenges. At present, mostly single stimuli like temperature, water, and light are frequently employed in switching their shapes. However, these stimuli may not be suitable for all the applications. To overcome this, the development of multi stimuli-responsive and multi-functional SMPs are essential. Extensive research is progressing to develop an effective enzymatic or extra cellular matrix triggered SMPs to specifically target affected tissues. SMPs should be designed to overcome limitations such as loss of shape memory due to humidity, UV light exposure or any other external factors. Furthermore, designing a biodegradable material to complement the tissue regeneration timeline is essential to develop the personalized tissue implants for cardiac, bone tissue and other tissue specific constructs. The drug delivery with SMPs can significantly enhance its potential by incorporating nanotechnology. At present SMPs are mostly utilized to deliver one therapeutic drug agent. However, they have potential to load and deliver multiple drugs (and diagnostic molecules) sequentially. Hence, they can be suitable materials for combination therapy or theranostics. The limitations such as, sudden collapse of the stents, stent thrombosis, post implant immunogenic reactions and pathogenic bacterial biofilm formation with regard to traditional biomedical devices



can be overturned by improving mechanical and functional properties of multimodal SMPs by fabricating polymer composition. This strategy involving multimodal SMPs will improve the effectiveness of stents for long term usage. Further, at present many SMPs utilized for 4D printing have high  $T_g$  or lack biodegradability (like epoxy resins), which limits its application in biological systems. To overcome these challenges SMPs should be designed with low  $T_g$  (25–40 °C), which enable them to be activated under physiologically relevant conditions. Furthermore, biodegradable and biocompatible polymeric materials should be incorporated in preparing SMPs, which will be crucial for biological studies. These advancements can potentially lead to design more efficient 4D printed materials for applications like nanorobotics, deployable devices, tissue scaffold and biomedical implants *etc.* Apart from biomedical applications, the properties of SMPs like shape memory and self-healing are also effective in designing the light weight deployable devices and repairing minor damages in the spacecrafts in response to external stimuli. SMPs can be designed to have a broad range of  $T_g$  (*e.g.* –150 °C to +150 °C) to sustain the thermal conditions in space. However, incorporation of multi stimuli responsiveness will provide precise control over shape transformations. To enhance the longevity in space, photo-resistant SMPs can be designed to withstand prolonged exposure to UV radiation and cosmic rays. This in turn will enhance spacecraft's performance. These advancements will lead to the development of innovative self-deploying systems, like unfolding in response to external stimuli, soft robotic grippers for sample collection, surface exploration *etc.* Additionally, SMPs have the advantage of recyclability and can be designed in such a way, even after repeated recycling they should be capable of retaining their mechanical properties. However, due to their complex structure and high cross-linking densities recycling is quite difficult and requires new age technology to reduce the degradation after recycling. In regard to wastewater treatment, SMPs are in early stage of research, but exhibiting significant capabilities to be smart, compatible devices to detect the multiple hazardous elements in water, even in remote areas. In future SMPs could be incorporated into portable water testing devices that serve as smart detecting and filtration systems, enabling quick detection and removal of pollutants. SMP-based textiles are assumed to play crucial role in developing next generation smart and adaptive wearables. For example, SMPs can be used to design smart garments for medical uses, adaptive protecting suits for astronauts, fire fighter and electricians. Further, SMPs based smart fabrics can be used to design specialized uniforms, that protects soldiers from harsh environmental conditions like extremely high or low temperature and sudden weather changes. The cost effective SMP-based garments could be well accepted for public use in daily life. These advancements will contribute to protect the environment and human health. Therefore, development of such smarter and versatile materials would revolutionize human lives for upcoming decades.

## Author contributions

Pravan Kumar Chandaka: formal analysis, investigation, resources, visualization, writing – original draft. Attreyee Das: resources, writing – original draft. Partha Laskar: conceptualization, investigation, methodology, resources, writing – original draft, supervision, funding acquisition. All authors have read and agreed to the final version of the manuscript.

## Conflicts of interest

There are no conflicts to declare.

## Data availability

The review does not contain any new unpublished data (*i.e.* primary research results, software, or code).

## Acknowledgements

Pravan Kumar Chandaka would like to thank the DST PURSE (SR/PURSE/2023/169(G) Dated 13/12/2023) for his fellowship. Attreyee Das would like to thank the GITAM Internship program (GITAM/RDC/RI-39/2024) for her fellowship. Partha Laskar would like to thank the GITAM SEED Grant (2024/0314), DST PURSE (SR/PURSE/2023/169(G) Dated 13/12/2023), and UGC-DAE CSR (CRS/2024-25/1761) for financial and research support.

## References

- C. Liu, H. Qin and P. T. Mather, Review of progress in shape-memory polymers, *J. Mater. Chem.*, 2007, **17**(16), 1543–1558.
- Q. Meng and J. Hu, A review of shape memory polymer composites and blends, *Composites, Part A*, 2009, **40**(11), 1661–1672.
- A. N. Patil and S. H. Sarje, Shape memory and shape recovery characterization of thermoplastic urethane, *Adv. Mater. Process. Technol.*, 2024, **6**, 1–6.
- Y. Q. Fu, W. M. Huang, J. K. Luo and H. Lu, Polyurethane shape-memory polymers for biomedical applications, in *InShape Memory Polymers for Biomedical Applications*, Woodhead Publishing, 2015, vol. 1, pp. 167–195.
- Y. Xia, Y. He, F. Zhang, Y. Liu and J. Leng, A review of shape memory polymers and composites: mechanisms, materials, and applications, *Adv. Mater.*, 2021, **33**(6), 2000713.
- Y. Hiruta, Poly(*N*-isopropylacrylamide)-based temperature- and pH-responsive polymer materials for application in biomedical fields, *Polym. J.*, 2022, **54**(12), 1419–1430.
- T. Chatterjee, P. Dey, G. B. Nando and K. Naskar, Thermo-responsive shape memory polymer blends based on alpha olefin and ethylene propylene diene rubber, *Polymer*, 2015, **78**, 180–192.
- T. Li, Y. Li, X. Wang, X. Li and J. Sun, Thermally and near-infrared light-induced shape memory polymers capable of healing mechanical damage and fatigued shape memory



- function, *ACS Appl. Mater. Interfaces*, 2019, **11**(9), 9470–9477.
- 9 Y. Guo, Z. Lv, Y. Huo, L. Sun, S. Chen, Z. Liu, C. He, X. Bi, X. Fan and Z. You, A biodegradable functional water-responsive shape memory polymer for biomedical applications, *J. Mater. Chem. B*, 2019, **7**(1), 123–132.
- 10 J. Hu, Y. Zhu, H. Huang and J. Lu, Recent advances in shape-memory polymers: structure, mechanism, functionality, modeling and applications, *Prog. Polym. Sci.*, 2012, **37**(12), 1720–1763.
- 11 S. N. Kurup, C. Ellingford and C. Wan, Shape memory properties of polyethylene/ethylene vinyl acetate/carbon nanotube composites, *Polym. Test.*, 2020, **81**, 106227.
- 12 A. Fulati, K. Uto and M. Ebara, Influences of crystallinity and crosslinking density on the shape recovery force in poly( $\epsilon$ -caprolactone)-based shape-memory polymer blends, *Polymers*, 2022, **14**(21), 4740.
- 13 M. Staszczak, K. M. Nabavian, K. M. Golasinski, L. Urbański, K. Takeda, R. Matsui and E. A. Pieczyńska, Characterization of polyurethane shape memory polymer and determination of shape fixity and shape recovery in subsequent thermomechanical cycles, *Polymers*, 2022, **14**(21), 4775.
- 14 X. Li, R. Yu, Y. He, Y. Zhang, X. Yang, X. Zhao and W. Huang, Four-dimensional printing of shape memory polyurethanes with high strength and recyclability based on Diels–Alder chemistry, *Polymer*, 2020, **200**, 122532.
- 15 Q. Zhao, H. J. Qi and T. Xie, Recent progress in shape memory polymer: New behavior, enabling materials, and mechanistic understanding, *Prog. Polym. Sci.*, 2015, **49**, 79–120.
- 16 H. Zhang, H. Wang, W. Zhong and Q. Du, A novel type of shape memory polymer blend and the shape memory mechanism, *Polymer*, 2009, **50**(6), 1596–1601.
- 17 T. Xiang, J. Hou, H. Xie, X. Liu, T. Gong and S. Zhou, Biomimetic micro/nano structures for biomedical applications, *Nano Today*, 2020, **35**, 100980.
- 18 W. Zhao, C. Yue, L. Liu, Y. Liu and J. Leng, Research progress of shape memory polymer and 4D printing in biomedical application, *Adv. Healthcare Mater.*, 2023, **12**(16), 2201975.
- 19 A. Maroni, A. Melocchi, L. Zema, A. Foppoli and A. Gazzaniga, Retentive drug delivery systems based on shape memory materials, *J. Appl. Polym. Sci.*, 2020, **137**(25), 48798.
- 20 T. Li, L. Chen, Y. Yuan and R. Shi, The current status, prospects, and challenges of shape memory polymers application in bone tissue engineering, *Polymers*, 2023, **15**(3), 556.
- 21 A. Singhwani, A. Jaiswal, K. Chaturvedi, M. Mili, K. Pal, R. K. Mohapatra, M. A. Khan, H. N. Bhargava, A. K. Srivastava and S. Verma, Smart shape memory polymers and their significance in biomedical applications: a review, *Polym. Adv. Technol.*, 2023, **34**(11), 3552–3568.
- 22 A. Yadav, S. K. Singh, S. Das, S. Kumar and A. Kumar, Shape memory polymer and composites for space applications: a review, *Polym. Compos.*, 2025, 1–37.
- 23 Y. Zheng, Y. Du, L. Chen, W. Mao, Y. Pu, S. Wang and D. Wang, Recent advances in shape memory polymeric nanocomposites for biomedical applications and beyond, *Biomater. Sci.*, 2024, **12**(8), 2033–2040.
- 24 Y. Ikada, Challenges in tissue engineering, *J. R. Soc. Interface*, 2006, **3**(10), 589–601.
- 25 R. S. Langer and J. P. Vacanti, Tissue engineering: the challenges ahead, *Sci. Am.*, 1999, **280**(4), 86–89.
- 26 N. Sood, A. Bhardwaj, S. Mehta and A. Mehta, Stimuli-responsive hydrogels in drug delivery and tissue engineering, *Drug Delivery*, 2016, **23**(3), 748–770.
- 27 C. M. Yakacki, R. Shandas, C. Lanning, B. Rech, A. Eckstein and K. Gall, Unconstrained recovery characterization of shape-memory polymer networks for cardiovascular applications, *Biomaterials*, 2007, **28**(14), 2255–2263.
- 28 R. T. Tran, J. Yang and G. A. Ameer, Citrate-based biomaterials and their applications in regenerative engineering, *Ann. Rev. Mater. Res.*, 2015, **45**(1), 277–310.
- 29 A. Mahdavi, L. Ferreira, C. Sundback, J. W. Nichol, E. P. Chan, D. J. Carter, C. J. Bettinger, S. Patavanich, L. Chignozha, E. Ben-Joseph and A. Galakatos, A biodegradable and biocompatible gecko-inspired tissue adhesive, *Proc. Natl. Acad. Sci. U. S. A.*, 2008, **105**(7), 2307–2312.
- 30 V. Schwach and R. Passier, Native cardiac environment and its impact on engineering cardiac tissue, *Biomater. Sci.*, 2019, **7**(9), 3566–3580.
- 31 M. Bao, X. Lou, Q. Zhou, W. Dong, H. Yuan and Y. Zhang, Electrospun biomimetic fibrous scaffold from shape memory polymer of PDLA-co-TMC for bone tissue engineering, *ACS Appl. Mater. Interfaces*, 2014, **6**(4), 2611–2621.
- 32 H. Ramaraju, L. D. Solorio, M. L. Bocks and S. J. Hollister, Degradation properties of a biodegradable shape memory elastomer, poly(glycerol dodecanoate), for soft tissue repair, *PLoS ONE*, 2020, **15**(2), e0229112.
- 33 J. Feng, H. Shi, X. Yang and S. Xiao, Self-adhesion conductive sub-micron fiber cardiac patch from shape memory polymers to promote electrical signal transduction function, *ACS Appl. Mater. Interfaces*, 2021, **13**(17), 19593–19602.
- 34 C. Du, J. Liu, D. A. Fikhman, K. S. Dong and M. B. Monroe, Shape memory polymer foams with phenolic acid-based antioxidant and antimicrobial properties for traumatic wound healing, *Front. Bioeng. Biotechnol.*, 2022, **10**, 809361.
- 35 M. Ramezani and M. B. Monroe, Bacterial protease-responsive shape memory polymers for infection surveillance and biofilm inhibition in chronic wounds, *J. Biomed. Mater. Res. A*, 2023, **111**(7), 921–937.
- 36 G. Tiwari, R. Tiwari, B. Sriwastawa, L. Bhati, S. Pandey, P. Pandey and S. K. Bannerjee, Drug delivery systems: an updated review, *Int. J. Pharm. Invest.*, 2012, **2**(1), 2.
- 37 H. Wen, H. Jung and X. Li, Drug delivery approaches in addressing clinical pharmacology-related issues:



- opportunities and challenges, *AAPS J.*, 2015, **17**(6), 1327–1340.
- 38 A. Raza, T. Rasheed, F. Nabeel, U. Hayat, M. Bilal and H. M. Iqbal, Endogenous and exogenous stimuli-responsive drug delivery systems for programmed site-specific release, *Molecules*, 2019, **24**(6), 1117.
- 39 J. K. Patra, G. Das, L. F. Fraceto, E. V. Campos, M. D. Rodriguez-Torres, L. S. Acosta-Torres, L. A. Diaz-Torres, R. Grillo, M. K. Swamy, S. Sharma and S. Habtemariam, Nano based drug delivery systems: recent developments and future prospects, *J. Nanobiotechnol.*, 2018, **16**(1), 71.
- 40 S. Somani, P. Laskar, N. Altwaijry, P. Kewcharoenpong, C. Irving, G. Robb, B. S. Pickard and C. Dufès, PEGylation of polypropylenimine dendrimers: effects on cytotoxicity, DNA condensation, gene delivery and expression in cancer cells, *Sci. Rep.*, 2018, **8**(1), 9410.
- 41 P. Laskar, S. Somani, S. J. Campbell, M. Mullin, P. Keating, R. J. Tate, C. Irving, H. Y. Leung and C. Dufès, Camptothecin-based dendrimersomes for gene delivery and redox-responsive drug delivery to cancer cells, *Nanoscale*, 2019, **11**(42), 20058–20071.
- 42 P. Laskar, S. Somani, N. Altwaijry, M. Mullin, D. Bowering, M. Warzecha, P. Keating, R. J. Tate, H. Y. Leung and C. Dufès, Redox-sensitive, cholesterol-bearing PEGylated poly(propylene imine)-based dendrimersomes for drug and gene delivery to cancer cells, *Nanoscale*, 2018, **10**(48), 22830–22847.
- 43 P. Laskar, S. Samanta, S. K. Ghosh and J. Dey, *In vitro* evaluation of pH-sensitive cholesterol-containing stable polymeric micelles for delivery of camptothecin, *J. Colloid Interface Sci.*, 2014, **430**, 305–314.
- 44 P. Laskar, J. Dey and S. kumar Ghosh, Evaluation of zwitterionic polymersomes spontaneously formed by pH-sensitive and biocompatible PEG based random copolymers as drug delivery systems, *Colloids Surf., B*, 2016, **139**, 107–116.
- 45 P. Laskar, A. Dhasmana, S. Kotnala, M. Jaggi, M. M. Yallapu and S. C. Chauhan, Glutathione-responsive tannic acid-assisted FRET nanomedicine for cancer therapy, *Pharmaceutics*, 2023, **15**(5), 1326.
- 46 K. Maeyouf, I. Sakpakdeejaroen, S. Somani, J. Meewan, H. Ali-Jerman, P. Laskar, M. Mullin, G. MacKenzie, R. J. Tate and C. Dufès, Transferrin-bearing, zein-based hybrid lipid nanoparticles for drug and gene delivery to prostate cancer cells, *Pharmaceutics*, 2023, **15**(11), 2643.
- 47 P. Laskar, B. Saha, S. K. Ghosh and J. Dey, PEG based random copolymer micelles as drug carriers: the effect of hydrophobe content on drug solubilization and cytotoxicity, *RSC Adv.*, 2015, **5**(21), 16265–16276.
- 48 J. Almowalad, P. Laskar, S. Somani, J. Meewan, R. J. Tate and C. Dufès, Lactoferrin-and dendrimer-bearing gold nanocages for stimulus-free DNA delivery to prostate cancer cells, *Int. J. Nanomed.*, 2022, **1**, 1409–1421.
- 49 S. Obuobi, H. K. Tay, N. D. Tram, V. Selvarajan, J. S. Khara, Y. Wang and P. L. Ee, Facile and efficient encapsulation of antimicrobial peptides *via* crosslinked DNA nanostructures and their application in wound therapy, *J. Controlled Release*, 2019, **313**, 120–130.
- 50 M. C. Serrano, L. Carbajal and G. A. Ameer, Novel biodegradable shape-memory elastomers with drug-releasing capabilities, *Adv. Mater.*, 2011, **23**(19), 2211–2215.
- 51 S. R. Garfin, H. A. Yuan and M. A. Reiley, New technologies in spine: kyphoplasty and vertebroplasty for the treatment of painful osteoporotic compression fractures, *Spine*, 2001, **26**(14), 1511–1515.
- 52 M. Bil, E. Kijeńska-Gawrońska, E. Głodkowska-Mrówka, A. Manda-Handzlik and P. Mrówka, Design and *in vitro* evaluation of electrospun shape memory polyurethanes for self-fitting tissue engineering grafts and drug delivery systems, *Mater. Sci. Eng., C*, 2020, **110**, 110675.
- 53 S. Nayak, S. R. Prasad, D. Mandal and P. Das, Hybrid DNA-carbon dot-poly(vinylpyrrolidone) hydrogel with self-healing and shape memory properties for simultaneous trackable drug delivery and visible-light-induced antimicrobial photodynamic inactivation, *ACS Appl. Bio Mater.*, 2020, **3**(11), 7865–7875.
- 54 S. Ouchi, E. Niiyama, K. Sugo, K. Uto, S. Takenaka, A. Kikuchi and M. Ebara, Shape-memory balloon offering simultaneous thermo/chemotherapies to improve anti-osteosarcoma efficacy, *Biomater. Sci.*, 2021, **9**(20), 6957–6965.
- 55 A. U. Vakil, M. Ramezani and M. B. Monroe, Magnetically actuated shape memory polymers for on-demand drug delivery, *Materials*, 2022, **15**(20), 7279.
- 56 W. Zhou, X. Yu, Z. Zhang, X. Zou, H. Song and W. Zheng, Preparation and evaluation of luteolin-loaded PLA-based shape memory gastroretentive drug delivery systems, *Int. J. Pharm.*, 2024, **650**, 123670.
- 57 R. Xiao and W. M. Huang, Heating/solvent responsive shape-memory polymers for implant biomedical devices in minimally invasive surgery: current status and challenge, *Macromol. Biosci.*, 2020, **20**(8), 2000108.
- 58 R. A. Morgan, I. Loftus, L. Ratnam, R. Das, L. Mailli, M. S. Hamady and K. Lobotesis, Clinical experience with a shape memory polymer peripheral vascular embolisation plug: a case series, *CVIR Endovasc.*, 2021, **4**(1), 29.
- 59 M. Y. Emmert, A. Venbrux, L. Rudakov, N. Cesarovic, M. G. Radvany, P. Gailloud, V. Falk and A. Plass, The endovascular occlusion system for safe and immediate peripheral vessel occlusion during vascular interventions, *Interact. Cardiovasc. Thorac. Surg.*, 2013, **17**(5), 882–885.
- 60 C. M. Yakacki, R. Shandas, C. Lanning, B. Rech, A. Eckstein and K. Gall, Unconstrained recovery characterization of shape-memory polymer networks for cardiovascular applications, *Biomaterials*, 2007, **28**(14), 2255–2263.
- 61 M. C. Chen, H. W. Tsai, Y. Chang, W. Y. Lai, F. L. Mi, C. T. Liu, H. S. Wong and H. W. Sung, Rapidly self-expandable polymeric stents with a shape-memory property, *Biomacromolecules*, 2007, **8**(9), 2774–2780.
- 62 S. H. Ajili, N. G. Ebrahimi and M. Soleimani, Polyurethane/polycaprolactane blend with shape memory effect as



- a proposed material for cardiovascular implants, *Acta Biomater.*, 2009, 5(5), 1519–1530.
- 63 R. Xiao and T. D. Nguyen, Modeling the solvent-induced shape-memory behavior of glassy polymers, *Soft Matter*, 2013, 9(39), 9455–9464.
- 64 Y. S. Wong, A. V. Salvekar, K. Da Zhuang, H. Liu, W. R. Birch, K. H. Tay, W. M. Huang and S. S. Venkatraman, Bioabsorbable radiopaque water-responsive shape memory embolization plug for temporary vascular occlusion, *Biomaterials*, 2016, 102, 98–106.
- 65 W. Small, P. R. Buckley, T. S. Wilson, W. J. Bennett, J. Hartman, D. Saloner and D. J. Maitland, Shape memory polymer stent with expandable foam: a new concept for endovascular embolization of fusiform aneurysms, *IEEE Trans. Biomed. Eng.*, 2007, 54(6), 1157–1160.
- 66 J. N. Rodriguez, F. J. Clubb, T. S. Wilson, M. W. Miller, T. W. Fossum, J. Hartman, E. Tuzun, P. Singhal and D. J. Maitland, In vivo response to an implanted shape memory polyurethane foam in a porcine aneurysm model, *J. Biomed. Mater. Res. A*, 2014, 102(5), 1231–1242.
- 67 Y. Zhang, N. Zheng, Y. Cao, F. Wang, P. Wang, Y. Ma, B. Lu, G. Hou, Z. Fang, Z. Liang and M. Yue, Climbing-inspired twining electrodes using shape memory for peripheral nerve stimulation and recording, *Sci. Adv.*, 2019, 5(4), eaaw1066.
- 68 T. Ware, D. Simon, D. E. Arreaga-Salas, J. Reeder, R. Rennaker, E. W. Keefer and W. Voit, Fabrication of responsive, softening neural interfaces, *Adv. Funct. Mater.*, 2012, 22(16), 3470–3479.
- 69 C. Chen, J. Hu, H. Huang, Y. Zhu and T. Qin, Design of a smart nerve conduit based on a shape-memory polymer, *Adv. Mater. Technol.*, 2016, 1(4), 1600015.
- 70 J. Wang, H. Xiong, T. Zhu, Y. Liu, H. Pan, C. Fan, X. Zhao and W. W. Lu, Bioinspired multichannel nerve guidance conduit based on shape memory nanofibers for potential application in peripheral nerve repair, *ACS Nano*, 2020, 14(10), 12579–12595.
- 71 Y. Zhang, L. Huang, H. Song, C. Ni, J. Wu, Q. Zhao and T. Xie, 4D printing of a digital shape memory polymer with tunable high performance, *ACS Appl. Mater. Interfaces*, 2019, 11(35), 32408–32413.
- 72 M. Bodaghi, A. R. Damanpack and W. H. Liao, Triple shape memory polymers by 4D printing, *Smart Mater. Struct.*, 2018, 27(6), 065010.
- 73 C. A. Spiegel, M. Hackner, V. P. Bothe, J. P. Spatz and E. Blasco, 4D printing of shape memory polymers: from macro to micro, *Adv. Funct. Mater.*, 2022, 32(51), 2110580.
- 74 Y. Y. Choong, S. Maleksaedi, H. Eng, J. Wei and P. C. Su, 4D printing of high performance shape memory polymer using stereolithography, *Mater. Des.*, 2017, 126, 219–225.
- 75 Q. Ge, A. H. Sakhaei, H. Lee, C. K. Dunn, N. X. Fang and M. L. Dunn, Multimaterial 4D printing with tailorable shape memory polymers, *Sci. Rep.*, 2016, 6(1), 31110.
- 76 P. C. Chen, T. T. Saha, A. M. Smith and R. C. Romeo, Progress in very lightweight optics using graphite fiber composite materials, *Opt. Eng.*, 1998, 37(2), 666–676.
- 77 P. C. Chen, C. W. Bowers, D. A. Content, J. Marzouk and R. C. Romeo, Advances in very lightweight composite mirror technology, *Opt. Eng.*, 2000, 39(9), 2320–2329.
- 78 A. A. Abusafieh, D. R. Federico, S. J. Connell, E. J. Cohen and P. B. Willis, Dimensional stability of CFRP composites for space-based reflectors, *Optomech. Des. Eng.*, 2001, 4444, 9–16.
- 79 G. Ming, L. Liu, Y. Liu and J. Leng, Space deployable parabolic reflector based on shape memory polymer composites, *Compos. Struct.*, 2023, 304, 116327.
- 80 D. Kang, J. M. Jeong, K. I. Jeong and S. S. Kim, Improving the deformability and recovery moment of shape memory polymer composites for bending actuators: multiple neutral axis skins and deployable core, *ACS Appl. Mater. Interfaces*, 2023, 15(28), 33944–33956.
- 81 L. Luo, F. Zhang, W. Pan, Y. Yao, Y. Liu and J. Leng, Shape memory polymer foam: active deformation, simulation and validation of space environment, *Smart Mater. Struct.*, 2022, 31(3), 035008.
- 82 T. D. Dao, N. S. Ha, N. S. Goo and W. R. Yu, Design, fabrication, and bending test of shape memory polymer composite hinges for space deployable structures, *J. Intell. Mater. Syst. Struct.*, 2018, 29(8), 1560–1574.
- 83 H. M. Herath, J. A. Epaarachchi, M. M. Islam and J. Leng, Carbon fibre reinforced shape memory polymer composites for deployable space habitats, *Eng. J. Inst. Eng.*, 2019, 52(1), 1–9.
- 84 K. Hamad, M. Kaseem and F. Deri, Recycling of waste from polymer materials: an overview of the recent works, *Polym. Degrad. Stab.*, 2013, 98(12), 2801–2812.
- 85 J. Datta and P. Koczyńska, From polymer waste to potential main industrial products: Actual state of recycling and recovering, *Crit. Rev. Environ. Sci. Technol.*, 2016, 46(10), 905–946.
- 86 I. A. Ignatyev, W. Thielemans and B. Vander Beke, Recycling of polymers: a review, *ChemSusChem*, 2014, 7(6), 1579–1593.
- 87 G. Crini and E. Lichtfouse, Advantages and disadvantages of techniques used for wastewater treatment, *Environ. Chem. Lett.*, 2019, 17(1), 145–155.
- 88 A. Sonune and R. Ghate, Developments in wastewater treatment methods, *Desalination*, 2004, 167, 55–63.
- 89 G. W. De Kort, L. H. Bouvrie, S. Rastogi and C. H. Wilsens, Thermoplastic PLA-LCP composites: a route toward sustainable, reprocessable, and recyclable reinforced materials, *ACS Sustain. Chem. Eng.*, 2019, 8(1), 624–631.
- 90 S. Wang, Y. Yang, H. Ying, X. Jing, B. Wang, Y. Zhang and J. Cheng, Recyclable, self-healable, and highly malleable poly (urethane-urea) s with improved thermal and mechanical performances, *ACS Appl. Mater. Interfaces*, 2020, 12(31), 35403–35414.
- 91 N. Zheng, Y. Xu, Q. Zhao and T. Xie, Dynamic covalent polymer networks: a molecular platform for designing functions beyond chemical recycling and self-healing, *Chem. Rev.*, 2021, 121(3), 1716–1745.
- 92 W. Du, Y. Jin, L. Shi, Y. Shen, S. Lai and Y. Zhou, NIR-light-induced thermoset shape memory polyurethane



## Review

- composites with self-healing and recyclable functionalities, *Composites, Part B*, 2020, **195**, 108092.
- 93 S. Zhang, B. Qin, J. F. Xu and X. Zhang, Multi-recyclable shape memory supramolecular polyurea with long cycle life and superior stability, *ACS Mater. Lett.*, 2021, **3**(4), 331–336.
- 94 N. Gogoi, M. Barooah, G. Majumdar and D. Chowdhury, Carbon dots rooted agarose hydrogel hybrid platform for optical detection and separation of heavy metal ions, *ACS Appl. Mater. Interfaces*, 2015, **7**(5), 3058–3067.
- 95 D. Kim, J. Kim, S. Jo and T. S. Lee, Colorimetric detection of Co ions by a poly(vinyl alcohol)-based hydrogel using color coordinate, *Dyes Pigm.*, 2022, **197**, 109894.
- 96 L. Bertolacci, P. Valentini and P. P. Pompa, A nanocomposite hydrogel with catalytic properties for trace-element detection in real-world samples, *Sci. Rep.*, 2020, **10**(1), 18340.
- 97 M. Wang, L. Shao and M. Jia, Shape memory and underwater superelastic mof@cellulose aerogels for rapid and large-capacity adsorption of metal ions, *Cellulose*, 2022, **29**(15), 8243–8254.
- 98 M. Li, R. Chen, Q. Yang, W. Yang, C. Qin, H. Song, L. Zhang and W. Chen, An economic naked-eye visualization detection of heavy metal ions using a shape memory hydrogel, *Ind. Eng. Chem. Res.*, 2024, **63**(43), 18289–18297.
- 99 K. Lacasse and W. Baumann, *Textile Chemicals: Environmental Data and Facts*, Springer Science & Business Media, 2012.
- 100 J. Charbonnet, J. E. Lawrence, L. E. Rubin and S. A. Tepfer, New approaches in cotton crosslinking, *Greener Solutions*, 2013, 1–71.
- 101 M. O. Gök, M. Z. Bilir and B. H. Gürcüm, Shape-memory applications in textile design, *Proc. Soc. Behav. Sci.*, 2015, **195**, 2160–2169.
- 102 J. Zou, Y. Wang, X. Yu, R. Liu, W. Fan, J. Cheng and W. Cai, Skin-inspired zero carbon heat-moisture management based on shape memory smart fabric, *Adv. Fiber Mater.*, 2024, **15**, 1–20.
- 103 X. Zhang, Y. Gu, X. Chao, Z. Wang, S. Wu, J. Xu, Z. Li, M. Pan and D. Shou, All-weather 3D self-folding fabric for adaptive personal thermoregulation, *Nano-Micro Lett.*, 2025, **17**(1), 290.

